Chitosan tubes of varying degrees of acetylation for bridging peripheral nerve defects

Haastert-Talini, Kirsten; Geuna, Stefano; Dahlin, Lars; Meyer, Cora; Stenberg, Lena; Freier, Thomas; Heimann, Claudia; Barwig, Christina; Pinto, Luis F. V.; Raimondo, Stefania; Gambarotta, Giovanna; Samy, Silvina Ribeiro; Sousa, Nuno; Salgado, Antonio J.; Ratzka, Andreas; Wrobel, Sandra; Grothe, Claudia

Published in:
Biomaterials

DOI:
10.1016/j.biomaterials.2013.08.074

2013

Biomaterials 34 (2013) 9886–9904

Contents lists available at ScienceDirect

Biomaterials

journal homepage: www.elsevier.com/locate/biomaterials

Chitosan tubes of varying degrees of acetylation for bridging peripheral nerve defects

Kirsten Haastert-Talini [a, b], Stefano Geuna [c], Lars B. Dahlin [d], Cora Meyer [a, b], Lena Stenberg [d], Thomas Freier [e], Claudia Heimann [e], Christina Barwig [e], Luis F.V. Pinto [f], Stefania Raimondo [c], Giovanna Gambarotta [c], Silvina Ribeiro Samy [g, h], Nuno Sousa [g, h], Antonio J. Salgado [g, h], Andreas Ratzka [a], Sandra Wrobel [a, b], Claudia Grothe [a, b, *]

[a] Institute of Neuroanatomy, Hannover Medical School, Hannover, Germany
[b] Center for Systems Neuroscience (ZSN), Hannover, Germany
[c] Department of Clinical and Biological Sciences, and Cavalieri Ottolenghi Neuroscience Institute, University of Turin, Turin, Italy
[d] Hand Surgery Department of Clinical Sciences Malmö – Hand Surgery, Skåne University Hospital, Lund University, Malmö, Sweden
[e] Medovent GmbH, Mainz, Germany
[f] Altakitin S.A., Portugal
[g] Life and Health Sciences Research Institute (ICVS), School of Health Sciences, University of Minho, Braga, Portugal
[h] ICVS/3B's, PT Government Associate Lab., Braga, Guimarães, Portugal

ARTICLE INFO

Article history:
Received 1 August 2013
Accepted 27 August 2013
Available online 17 September 2013

Keywords:
Chitosan
Nerve guide
Electrophysiology
Histomorphometry
Connective tissue
Degradation

ABSTRACT

Biosynthetic nerve grafts are desired as alternative to autologous nerve grafts in peripheral nerve reconstruction. Artificial nerve conduits still have their limitations and are not widely accepted in the clinical setting. Here we report an analysis of fine-tuned chitosan tubes used to reconstruct 10 mm nerve defects in the adult rat. The chitosan tubes displayed low, medium and high degrees of acetylation (DAI: ~2%, DA: ~5%, DAIII: ~20%) and therefore different degradability and microenvironments for the regenerating nerve tissue. Short and long term investigations were performed demonstrating that the chitosan tubes allowed functional and morphological nerve regeneration similar to autologous nerve grafts. Irrespective of the DA growth factor regulation demonstrated to be the same as in controls. Analyses of stereological parameters as well as the immunological tissue response at the implantation site and in the regenerated nerves, revealed that DAI and DAIII chitosan tubes displayed some limitations in the support of axonal regeneration and a high speed of degradation accompanied with low mechanical stability, respectively. The chitosan tubes combine several pre-requisites for a clinical acceptance and DAII chitosan tubes have to be judged as the most supportive for peripheral nerve regeneration.

1. Introduction

In general, peripheral nerves have the ability to regenerate following nerve lesion in contrast to the central nervous system. However, in cases of more complex injuries with substantial loss of nerve tissue and a subsequent defect between the nerve ends, the requirements for axonal regeneration are not sufficiently fulfilled. Such complex peripheral nerve injuries, which include 300,000 cases per year in Europe due to traumatic events, represent a major cause for morbidity and disability. During the last decades considerable efforts have been made to support and improve peripheral nerve regeneration across a nerve defect, but with limited and minor success [1]. Therefore, despite several shortcomings and limitations, such as misdirection of regenerating axons, neuronal cell death, and donor site morbidity, the gold standard for bridging a nerve defect remains grafting of an autologous nerve transplant to overcome such large defects [2]. The purpose is to apply an adequate substrate, including the provision of trophic and tropic factors, for the regrowing axons in order to restore the function after reconstruction of the nerve defect [3].

As a possible alternative for autologous nerve grafts, a variety of materials have been tested with regard to their suitability for fabrication of synthetic nerve conduits for bridging nerve defects [4]. In

* Corresponding author. Institute of Neuroanatomy, Hannover Medical School, Carl-Neuberg-Str. 1, 30625 Hannover, Germany. Fax: +49 511 532 2880.
E-mail address: Grothe.Claudia@mh-hannover.de (C. Grothe).

0142-9612
http://dx.doi.org/10.1016/j.biomaterials.2013.08.074

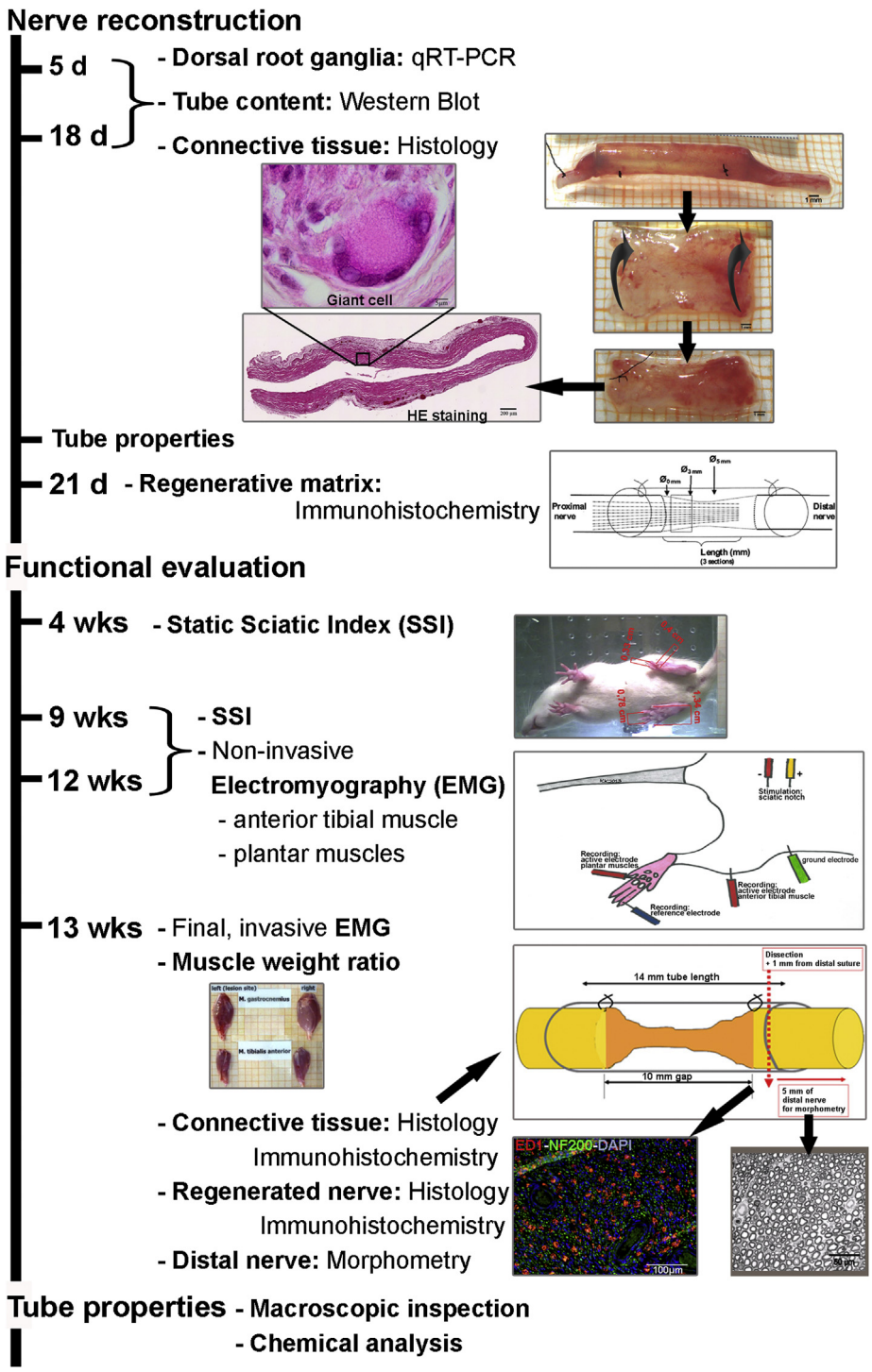

Fig. 1. Illustration of the various components of the comprehensive in vivo analysis of the new chitosan tubes with different degrees of acetylation as performed by several partners of the BIOHYBRID consortium. After the short terms of 5 and 18 days after nerve reconstruction, the connective tissue surrounding the chitosan tubes, the properties of the tubes, tube content as well as the proximal nerve ends and corresponding dorsal root ganglia were assessed with different methods, including RT-PCR, Western Blot, histology and immunohistochemistry. After 21 days in vivo, the newly formed regenerative matrix and the distal nerve segments were evaluated for matrix dimension, length of axonal outgrowth, and numbers of activated and apoptotic Schwann cells and total number of DAPI stained cells in the matrix and in the distal nerve segments. In long term observation, assessments of the motor regeneration were performed including the static sciatic index calculation, non-invasive and invasive electrodiagnostical measurements and muscle weight evaluation. Histological analyses were performed with the connective tissue and the regenerated nerve tissue. Finally, distal nerve morphometry and detailed analyses of the tube properties after nerve reconstruction and explantation were performed.

addition to non-degradable silicone tubes, which were earlier used clinically as an alternative for nerve repair [5,6] several biodegradable materials have been developed in animal experiments and applied for clinical investigation of nerve reconstruction devices [1,4]. Conduits, which are approved by the Food and Drug Administration (FDA) and authorized by the EC respectively, include Neurotube™ poly(glycolide) (PGA) tubes (successfully used in the clinical repair of digital nerves with defects of up to 3 cm in length [7]), Neura-Gen™ collagen nerve tubes [8,9], and Neurolac™ tubes [10,11]. Furthermore, processed, i.e. extracted, nerve allografts have

also been approved and applied to reconstruct nerve defects [12]. Although these off-the-shelve products have unlimited supply and avoid donor site morbidity, they have serious limitations in supporting peripheral nerve regeneration. Functional outcome after their use for nerve reconstruction is highly variable and only comparable to autologous nerve grafting when short defects in small diameter nerves are to be reconstructed [2,13]. Until today, no tubular or other type of biosynthetic nerve graft has shown strong potential to replace autologous nerve grafting for reconstruction of the substantial human nerves, such as the median or ulnar nerve trunks [14].

During the last years, the natural biopolymer chitosan – a derivative of chitin – has gained increasing interest in biomedical and tissue engineering applications. Chitosan displays biocompatibility, biodegradability, low toxicity, and structural similarity to natural glycosaminoglycans. Recent in vitro studies revealed the suitability of chitosan membranes as substrate for survival and oriented Schwann cell growth [12] as well as survival and differentiation of neuronal cells [15,16]. In addition, chitosan tubes alone or in combination with other biomaterials can efficiently bridge peripheral nerve defects [4,17]. However, improved technologies have been developed to overcome the poor mechanical strength of chitosan tubes, which was one of the main factors limiting the use of such tubes as nerve guidance channels for clinical applications until now [18]. Moreover, optimal biodegradation and cell compatibility, which are important features for tissue engineering, had to be adjusted by different degrees of acetylation of the chitosan [15].

The aim of the present study was to conduct in a multidisciplinary approach a comprehensive evaluation of chitosan tubes displaying different degrees of acetylation. The chitosan tubes were used to bridge a 10 mm defect in rat sciatic nerves. In addition to the fine-tuned manufacturing of the chitosan tubes and their evaluation with regard to biocompatibility, short and long term in vivo studies were performed and a battery of parameters were analysed. Thereby not only focussing on the effects on morphological and functional peripheral nerve regeneration, but also validating putative side effects, like Schwann cell survival and expression of transcription factors, neurotrophic factor regulation as well as immunological reaction. Finally, the properties of the non-implanted chitosan tubes were compared in structural and chemical analyses to tubes after explantation from the nerve reconstruction site.

2. Materials and methods

2.1. Manufacturing of chitosan

Medical grade chitosan supplied by Altakitin S.A. (Lisbon, Portugal) with a molecular weight (MW) of 260 kDa and degree of acetylation (DA) of 90% was obtained from *Pandalus borealis* shrimp shells using standard conditions for chitin extraction and deacetylation, following ISO 13485 requirements and specifications. The purification method consisted in homogeneous washing (liquid/liquid extraction) of chitosan with EDTA and SDS for heavy metals and protein removal. After the extractions, the product was washed with deionized water and neutralized prior to lyophilisation. The product was analysed using several methods and techniques to attest compliance with internal standards for degree of acetylation, molecular weight, heavy metal content, protein content, endotoxins, bioburden, pH, ash content and apparent viscosity.

2.2. Determination of the degree of acetylation by nuclear magnetic resonance (NMR) spectroscopy

The samples (approx. 5 mg) were dissolved in 2% DCl in D_2O (v/v, Sigma–Aldrich, Germany). The fid signal was acquired at 70 °C and suppressing the solvent signal (pulse program zgpr). Analysis and integrations were performed in MestReNova software according to Ref. [19].

2.3. Analysis of the molecular weight by gel permeation chromatography (GPC)

The samples (approx. 5 mg) were dissolved in 1 ml of eluent (AcOH/AcONa buffer pH 4.5, Panreac, Spain) and filtered through a 0.45 microns filter prior to injection (100 µl). The chromatographs were obtained at room temperature with a flow rate of 1 ml/min. A Varian PL aquagel-OH MIXED bed column (Varian, France) was used and a refractive index detector. Previously a calibration curve was obtained by using Varian pullulan polysaccharides certified standards in the same chromatographic conditions.

2.4. Production of chitosan tubes

Chitosan tubes were manufactured by Medovent GmbH (Mainz, Germany) under ISO 13485 conditions from chitin tubes made by a proprietary extrusion process, followed by distinctive washing and hydrolysis steps to adjust the required low, medium and high degree of acetylation (DA). Chitosan tubes have therefore been classified into DAI tubes (low DA, ~2%), DAII tubes (medium DA, ~5%) and DAIII tubes (high DA, ~20%). Tubes were finally cut into the required lengths and sterilized by electron beam.

2.5. In vitro cytotoxicity tests

In order to assess the short term cytotoxicity of the developed chitosan tubes, both the Minimum essential medium (MEM) extraction and the MTS cell viability tests were performed with 24 h, 72 h, and 7 days of extraction period following the guidelines described before [20]. In all tests the ratio material weight to extraction fluid was constant and equal to 0.2 g/ml for chitosan tubes (DAI: ~2%, DAII: ~5%, DAIII: ~20%), while for latex (negative control for cell viability) the ratio of material outer surface to extraction fluid was 2.5 cm^2/ml. After each period the extracts were filtered through a 0.45 µm pore size filter. These assays are particularly suitable for assessing the possible toxic effect of leachables extracted from biomedical polymers. With the MEM extraction test changes in cell morphology and growth inhibition are evaluated, whereas the metabolic cell viability is determined with the MTS test. In both cases, latex extracts (same extraction periods) were used as negative controls, while standard culture medium was used as positive control for cell death.

2.5.1. Cell culture

For the present experiment P1 rat bone marrow Mesenchymal Stromal Cells (RBMSCs) were used, which had been isolated according to the protocol described earlier [21]. Upon isolation cells were expanded in alpha-MEM (Gibco, USA), supplemented with 10% foetal bovine serum (FBS, Biochrome, Portugal) and 1% of an antibiotic–antimycotic mixture (Gibco). For the MTS test ($n = 5$, 2×10^4 cells/well) and the MEM extraction ($n = 3$, 2×10^4 cells), RBMSCs were seeded in a 24 well plate for 72 h at 37 °C, in a 5% (v/v) CO_2 cell culture incubator, prior to extract incubation.

2.5.2. MTS test

72 h after cell seeding, culture medium was removed from the wells and an identical volume (500 µl) of extraction fluid was added. Cultures were then incubated with the extracts for 72 h after which their metabolic viability was assessed through the MTS test. This is based on the bioreduction of [3-(4,5-dimethylthiazol-2-yl)-5-(3carboxymethoxyphenyl)-2-(4-sulfophenyl)-2H-tetrazolium] (MTS, Promega, USA), into a brown formazan product by dehydrogenase enzymes. After extracts, positive and negative controls were removed, a mixture of DMEM with MTS (5:1 ratio) was added to each well. Cells were then incubated for 3 h at 37 °C in a 5% CO_2 cell culture incubator after which the O.D. was determined at 490 nm using a 96 well plate reader (Tecan Sunrise, Männedorf, Switzerland).

2.5.3. MEM extraction test

72 h after cell seeding, culture medium was removed from the wells and an identical volume (500 µl) of extraction fluid was added. Cultures were then incubated with the extracts for 72 h after which a live/death assay by staining live cells with calcein-AM and non-viable cells with propidium iodide was performed. Cultures were observed in fluorescence microscopy.

2.6. Experimental design

In order to comprehensively analyse the performance of the newly designed chitosan tubes of different DA in vivo, short term and long term observation periods were chosen. As illustrated in Fig. 1, nerve reconstruction with chitosan tubes was performed and samples were collected for molecular and histological analysis after 5 and 18 days. The initially formed regenerative matrix was analysed 21 days after nerve reconstruction with chitosan tubes (short term). During the long term observation over 3 months the progress of sciatic nerve regeneration was periodically monitored with several functional tests. Finally, a comprehensive histomorphometrical analysis of the regenerated nerve tissue and further evaluation of the macroscopic and chemical tube properties were performed.

2.7. Animals and surgical procedure

The in vivo studies were performed in two different laboratories [Dahlin lab at Lund University (ULUND), Sweden, and Grothe lab at Hannover Medical School (MHH), Germany] with different animal breeders and regimes for anaesthesia and analgesia due to different local animal protection rules. All animal experiments were approved by the local animal protection committees (animal ethics committee in

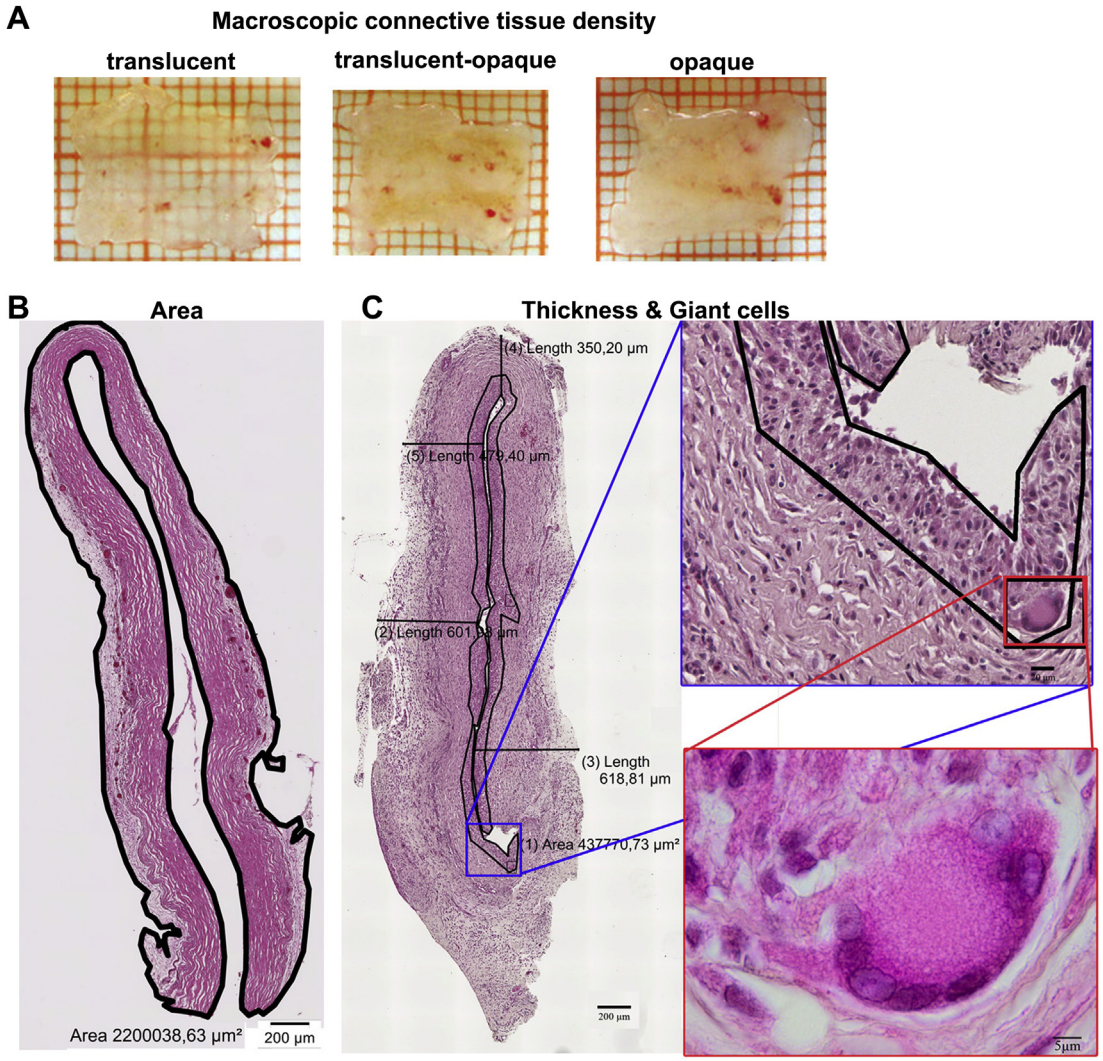

Fig. 2. Illustration of connective analysis. (A) Macroscopically three categories of optical density of the expanded connective tissue could be defined. (B) The area of sample connective tissue was determined in haematoxylin–eosin stained 7 µm paraffin cross sections. In these sections the inner surfaces of the connective tissue (contact area with chitosan tubes) are facing each other. (C) Within the contact area with the chitosan tubes the number of multinucleated giant cells (detail) was determined. Furthermore the thickness of sample connective tissue was evaluated at 5 randomly chosen locations.

Malmö/Lund, Sweden and animal care committee of Lower-Saxony, Germany). In common, female Wistar rats (225–250 g) were applied to the experiments and housed in groups of four animals under standard conditions (room temperature 22 ± 2 °C; humidity 55 ± 5%; light–dark-cycle 14-h/10-h [MHH] or 12-h/12-h [ULUND]) with food and water ad libitum.

For surgery, animals were anesthetized, sufficient analgesia induced and placed on a thermostatic blanket, to keep the body temperature stable, on the right side for surgery on the left sciatic nerves. After shaving the left hind leg the skin was disinfected, and aseptic techniques were used to ensure sterility. A skin incision was made with a surgical blade along the femur, and the gluteus and biceps femoris muscles were separated by sharp and blunt dissection to expose the sciatic nerve. The wound was kept open with the aid of small retractors. The sciatic nerve, exposed at the midthigh level, was transected with a single microscissors cut at a constant point (6 mm from the exit of the gluteus muscle). For tube transplantation 5 mm of the distal sciatic nerve end were removed and 14 mm long tubes were used to bridge a 10 mm nerve defect. Preparation of the tubes before nerve reconstruction included four washing steps in NaCl (4 × 30 min) as well as an overnight washing step. Four different observation periods were chosen after which the animals were finally examined and sacrificed prior to explantation of the implants and regenerated tissue: as short term periods 5 days (DAI, DAII, DAIII, $n = 6$ animals in each group), 18 days (DAI, DAII, DAIII, $n = 6$ animals in each group) and 21 days (DAI $n = 10$, DAII $n = 10$, DAIII $n = 9$); as long term period 3 months (13 weeks; DAI, DAII, DAIII, $n = 17$ animals in each group). Control animals for the long term investigations ($n = 17$) received an autologous nerve graft of 10 mm length, which was reversed (distal–proximal) and flipped 90° before three sutures (9-0, Ethilon) were placed 120° apart from each other. In control animals for the 5 days ($n = 4$) and 18 days ($n = 4$) short term investigations, the nerve defect was not reconstructed, but the proximal and distal nerve ends were folded over and sutured to themselves after removal of the 5 mm piece.

Anaesthesia at MHH was induced by chloral hydrate (370 mg/kg body weight, i.p., Sigma–Aldrich, Germany, MHH) combined with analgesia by buprenorphine (0.045 mg/kg body weight, Buprenovet, Germany). Anaesthesia at ULUND was induced by intraperitoneal injection of a mixture of Rompun (20 mg/ml; Bayer Health Care, Germany) and Ketalar (10 mg/ml, Pfizer, Finland). Postoperatively, all rats were treated with Temgesic (0.3 mg/ml; Schering-Plough Europe, Belgium) to prevent pain.

2.8. Quantitative RT-PCR

The ipsi- and contralateral dorsal root ganglia (DRGs) L3–L5 of animals subjected to the 5 and 18 days observation period were dissected and snap frozen in liquid nitrogen (5 days: DAI, DAII, DAIII $n = 3$ each, control $n = 4$; 18 days: DAI + DAIII $n = 3$ each, DAII + control $n = 4$ each). Tissue samples of each animal were homogenized and total RNA was extracted according to the manufacturer's instructions (RNeasy Plus Micro Kit, Qiagen, Germany). The eluate of 14 µl was used completely for cDNA synthesis using the iScript Kit (BioRad, Germany). Primer sequences were as previously stated for brain-derived neurotrophic factor (BDNF), growth-associated protein-43 (GAP-43) [22] and nerve growth factor (NGF) [23]. Further primer sequences were as follows: fibroblast growth factor-2 (FGF-2)-F: 5′-GAACCGGTACCTGGCTATGA-3′; FGF-2-R: 5′-CCAGGCGTTCAAAGAAGAAA-3′; interleukin 6 (IL6)-F: 5′-CGTTTCTACCTGGAGTTTGTGAAG-3′; IL6-R: 5′-GGAAGTTGGGG-TAGGAAGGAC-3′; tyrosine kinase receptor B (TrkB)-F: 5′-CCCAATTGTGGTCTGCCG-

3′; TrkB-R: 5′-CTTCCCTTCCTCCACCGTG-3′. Equal PCR efficiency was certified by serial cDNA dilutions and estimated to be 100%. Quantitative RT-PCR was performed with Power SYBR-Green PCR Master Mix (Applied Biosystems) on a StepOnePlus instrument (Applied Biosystems, Darmstadt, Germany) as described before [24]. Fold changes in mRNA levels are stated in comparison to the levels measured at the respective day on the contralateral side of the control animals. Calculation was done by using the $2(-\Delta\Delta Ct)$ method and normalized to the housekeeping gene peptidylprolyl isomerase A (Ppia)-F [24].

2.8.1. Western Blot

Tube contents were collected 5 and 18 days after nerve reconstruction with chitosan tubes and each pooled from 5 to 6 animals per DA. Samples were homogenized in 40 μl Radioimmunoprecipitation assay (RIPA) buffer (according to Ref. [25]). Samples were then boiled in Laemmli buffer (5 min) and separated by sodium dodecyl sulphate (SDS) polyacrylamide gel electrophoresis (PAGE) (12% gel) before being transferred (50 μg) electrophoretically to nitrocellulose membranes (Hybond ECL, Amersham) with 4 ng recombinant BDNF serving as positive control. Membranes were then probed with anti-BDNF (sc-546, 1:1000, rabbit, Santa Cruz, Germany) and anti-NGF (ab6199, 1:2000, abcam, UK) antibody and analysed following Ref. [25].

2.9. Assessment of the connective tissue

The connective tissue surrounding the tubes was macroscopically and histologically analysed. For the macroscopic evaluation, the connective tissue was dissected, spread on a scale paper glass plate and photographs taken of every sample. From the photographs, three classes of macroscopic connective tissue optical density were defined as translucent, translucent–opaque and opaque (Fig. 2A). Afterwards samples of the connective tissue ($n = 4$–6 per DA and evaluation time point), were folded and sutured at the proximal end such that the chitosan tubes contact surfaces were facing each other (Figs. 1 and 2B and C). The tissue was then fixed overnight in 4% paraformaldehyde (PFA) and paraffin embedded. For histological analysis blind-coded 7 μm paraffin sections were cut from the distal end of the connective tissue and subjected to haematoxylin–eosin (HE)-staining or immunohistochemistry for activated macrophages (see below) in the same sections. In 4–6 HE-stained sections per sample covering a distal–proximal distance of approximately 200 μm, the connective tissue area (Fig. 2B) and thickness (at 5 randomly chosen points, Fig. 2C) was determined. Furthermore, the number of multinucleated giant cells per mm^2 of the contact area with the chitosan tubes was manually quantified (Fig. 2C). Light microscopic evaluation (Olympus BX53 and Olympus BX51, Denmark) was aided by the programmes cellSense Dimensions and cellSense Entry (both Olympus; Denmark).

Immunohistochemistry was performed to estimate the number of ED1-stained cells, i.e. activated macrophages ($n = 4$–5/group). Therefore, two blind-coded 7 μm paraffin cross sections approximately 140 μm apart from each other were incubated in PBS + 5% rabbit serum as a blocking step prior to incubation with primary mouse anti-ED-1 antibody (1:1000; MCA 275R Serotec, UK) at 4 °C overnight. The next day sections were washed with PBS (3×) before being incubated with Alexa 555-conjugated secondary goat-anti-mouse antibody (1:1000; A21422, Invitrogen, Germany) for 1 h at room temperature (RT). Sections were finally counterstained with the nuclear dye 4′,6′-diamino-2-phenylindole (DAPI, 1:2000, Sigma, Germany) in PBS for 2 min at room temperature and then mounted with Moviol (Calbiochem, Germany, N° 475904). Two photomicrographs were each taken from an area with minimal and maximal ED1 signal per section (20× magnification) using an IX70 microscope (Olympus) and the cellP software (Olympus, Denmark) (Olympus). The number of ED1-+ cells was counted as number/mm^2 with the help of the ImageJ software (NIH, USA). The nuclear DAPI counterstaining was used to clearly identify ED1-immunopositive cells but not for further quantification in this case.

2.10. Analysis of regenerated matrix within the chitosan tubes at 21 days after nerve reconstruction

The sciatic nerve together with the chitosan tube and its content was harvested 21 days after surgery. The chitosan tube was removed, there after the tube content with proximal and distal nerve segments were fixed in Stefanini solution (4% paraformaldehyde and 1.9% picric acid in 0.1 M phosphate buffer pH 7.2) for 24 h. The samples were then washed in 0.01 M PBS pH 7.4 three times and stored in 20% sucrose solution overnight for cryoprotection. Before sectioning using a cryostat, the samples were embedded in OCT Compound (Tissue-Tek®, Histolab products AB, Gothenburg, Sweden) and frozen. The nerves sectioned longitudinally at 6 μm thickness were collected on Super Frost® plus glass slides (Menzel-Gläser, Germany).

2.10.1. Immunohistochemistry

Immunohistochemistry was performed for neurofilaments, activating transcription factor 3 (ATF3), and cleaved caspase 3 to evaluate axons, activated Schwann cells, and apoptotic Schwann cells, respectively, as described [26,27]. In short, the sections were washed in PBS for 5 min and incubated overnight at 4 °C with anti-human neurofilament protein (DAKO Glostrup, Denmark), diluted 1:80 in 0.25% Triton-X 100 and 0.25% BSA in PBS. The next day the slides were washed with PBS 3 × 5 min, then incubated for 1 h at room temperature with the secondary antibody ALEXA Fluor 594 conjugated goat anti-mouse IgG (Invitrogen, Molecular Probes, USA), diluted in 1:500 in PBS and coverslipped.

For ATF-3 immunohistochemistry, the sections were washed for 5 min in PBS and then incubated with rabbit anti-ATF-3 polyclonal antibody (1:200; Santa Cruz Biotechnology, USA), diluted 1:200 in 0.25% Triton-X 100 and 0.25% BSA in PBS, or with anti-cleaved caspase-3 antibody (1:200; Invitro Sweden AB, Stockholm, Sweden); both diluted in 0.25% Triton-X 100 and 0.25% BSA in PBS) overnight at 4 °C. The next day the slides were washed in PBS 3 × 5 min and then incubated with the secondary antibody Alexa Fluor 488 conjugated goat anti-rabbit IgG (Invitrogen, Molecular Probes, USA), diluted in 1:500 in PBS for 1 h at room temperature. Finally, the slides were washed 3 × 5 min in PBS, mounted with 4′,6′-diamino-2-phenylindole DAPI (Vectashield®, Vector Laboratories, Inc. Burlingame, USA) to visualize the oval shaped nuclei (i.e. for counting the total number of the cells) and then mounted and coverslipped.

The blind-coded sections were photomicrographed using a fluorescence microscope (Eclipse, Nikon, Tokyo, Japan) provided with a digital system camera (Nikon 80i) connected to a computer and the length of the outgrowing axons was measured from the site of lesion into the formed matrix in three randomly selected sections. The stained cells for cleaved caspase-3 and ATF-3 were also counted in one section (image size 500 × 400 μm) in the matrix 3 mm from the proximal nerve end (Fig. 1) and in the distal nerve segment as described [28]. The same squares were also used for counting the total number of DAPI stained cells. The images (20× magnification) were analysed with NIS elements (Nikon, Japan). Double staining for cleaved caspase 3 and S-100 was performed as described [27].

2.11. Functional evaluation

During the long term observation period of 3 months (13 weeks) after nerve reconstruction, the progress of functional motor recovery was monitored by calculation of the Static sciatic index, electrophysiological measurements (serial non-invasively and final invasively) and calculation of the lower limb muscle weight ratio. The investigators were blinded to the conditions of sciatic nerve reconstruction applied to the animals.

2.11.1. Static sciatic index (SSI)

The healthy SSI was determined 1 week prior to surgery and after surgery in weeks 1, 4, 9 and 12 as described before [29]. In brief, webcam images of the toe spreading of the right (contralateral) and left (ipsilateral) paw were acquired from the rats placed inside a plastic box located on a glass table. Using a freely available image-editing program (AxioVision, Zeiss, Jena, Germany), the distance between toe 1 and 5 (toe spread TS) as well as 2 and 4 (intermediate toe spread ITS) was measured for the lesioned (LTS; LITS) and non-lesioned (NTS; NITS) hind paws. The SSI was then calculated using the following equations (TSF = toe spread factor; ITSF = intermediate toe spread factor): $TSF = (LTS - NTS)/NTS$; $ITSF = (LITS - NITS)/NITS$; $SSI = (108.44 * TSF) + (31.85 * ITSF) - 5.49$.

2.11.2. Serial non-invasive electrodiagnostic recordings

For evaluation of ongoing muscle reinnervation in weeks 4, 9 and 12 after surgery a portable electrodiagnostic device (Keypoint Portable; Medtronic Functional Diagnostics A/S, Denmark) was used. Therefore, animals were anesthetized as described above and placed in a prone position and fixed with tape with the hindlimbs extended on a metal plate on top of a thermostatic blanket. Only during recordings the thermostatic blanket was turned off to avoid interfering signals. The sciatic nerve was stimulated with single electrical pulses (100 μs duration and supramaximal intensity) delivered by monopolar needles (30G, diameter 0.3 mm, length 10 mm; Alpine BioMed, Denmark) percutaneously placed either at the sciatic notch, proximal to the injury (proximal stimulation, cathode directly at sciatic notch, anode 1 cm more proximal) or in the popliteal fossa (distal stimulation). The compound muscle action potentials (CMAPs) of the tibialis anterior (TA) and plantar (PL) muscles were recorded by means of another pair of monopolar needles inserted across the skin on the muscle belly. To ensure reproducibility the recording needles were placed with the help of anatomical landmarks to secure the same placement on all animals. The active recording electrode is placed subcutaneously at the first third of the distance between knee and ankle on the TA muscle, and at the third metatarsal space for PL muscle recordings. The reference needle electrode was inserted at the distal phalange of the second or fourth toe. A ground needle electrode was inserted in the skin at the knee.

Taking into account the latency difference of the two stimulation points and the distance between them, the electrodiagnostic device calculated automatically the nerve conduction velocity (NCV). Furthermore, the signals amplitude and the area under the curve (AUC) of the negative CMAP peaks were recorded. Control values were obtained from the non-lesioned, right hindlimb.

2.11.3. Final invasive electrodiagnostic recordings

On the last day of observation (week 13) animals were once more anesthetized and the sciatic nerves were exposed consecutively on the lesioned and non-lesioned side. The recording electrodes were placed as described above. Using a bipolar steel

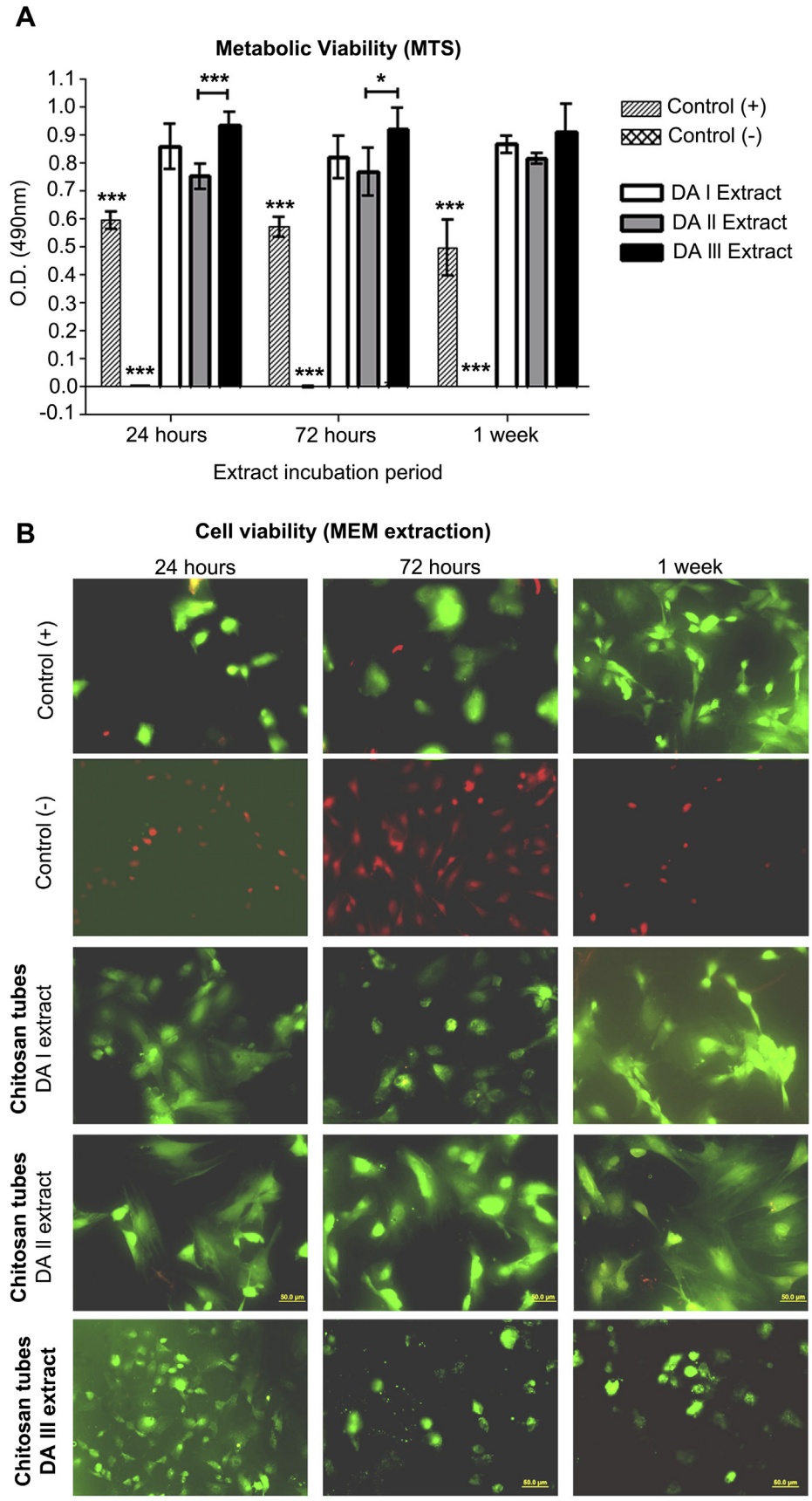

Fig. 3. (A) Metabolic activity of RBMSCs incubated with extracts from the chitosan tubes of different degrees of acetylation (DAI = ~2%; DAII = ~5%; DAIII = ~20%) for 72 h (MTS assay). No negative effect on the metabolic viability by any DA could be detected in comparison to the positive control. (B) Representative photomicrographs from the MEM extraction test. Incubation with the extracts from DAI-, DAII-, or DAIII-chitosan tubes did not negatively influence the cell density of cultured RBMSCs.

hook electrode the sciatic nerves were directly stimulated proximal and distal to the transplants [29]. Single electrical pulses (100 μs duration) with gradually increased intensity (not exceeding 8 mA) were applied in order to evaluate the threshold and maximal CMAP. Furthermore, the NCV was calculated by stimulating the sciatic nerve proximal and distal with a current intensity of 1 mA.

2.11.4. Muscle weight ratio

After completing the experiments the animals were sacrificed, the transplants with the adjacent nerve tissue were dissected and the gastrocnemius muscle and TA muscle of both hindlimbs were excised and weighted in order to determine the muscle weight ratio ($[g]_{ipsilateral}/[g]_{contralateral}$).

2.12. Histo-morphometrical assessment of the regenerated nerve tissue

The transplants with the adjacent nerve tissue were harvested and the regenerated nerve tissue extracted from the chitosan tubes. The regenerated nerve tissue was separated into a proximal and a distal part by a cut at 1 mm distal to the distal suture site (Fig. 1).

Five mm of the distal segment were then prepared for the stereological analysis (Fig. 1) by transferring the tissue into a fixative according to Karnovsky (2% PFA and 2.5% glutaraldehyde in 0.2 M sodium cacodylate buffer, pH 7.3) for 24 h, then rinsed three times with 0.1 M sodium cacodylate buffer containing 7.5% sucrose, prior to post-fixation in 1% OsO_4 for 2 h. Dehydration was performed in an ethyl alcohol row (5 × 5 min 25%, 5 × 5 min 50%, 5 × 5 min 75%). The samples were then shipped to the partner laboratory at the University in Turin for embedding in a mixture of Araldite resin (Sigma) following Glauerts' procedure [30].

The proximal regenerated nerve tissue was subjected to fixation in 4% PFA overnight at 4 °C. Afterwards Paraffin-embedding was performed in a Citadel tissue-embedding-automatic unit (Shandon Citadel 2000; USA) to prepare the tissue for HE-staining and immunohistochemical analysis.

2.12.1. Stereology/nerve morphometry

From each specimen of the distal nerve, 2.5 μm thick series of semi-thin transverse sections were cut using an Ultracut UCT ultramicrotome (Leica Microsystems, Germany). Finally, sections were stained using Toluidine blue and analysed with a DM4000B microscope equipped with a DFC320 digital camera and an IM50 image manager system (Leica Microsystems, Germany). Systematic random sampling and D-dissector were adopted, using a protocol previously described [31] in order to evaluate the total fibre number, fibre and axon diameter, myelin thickness and *g*-ratio.

2.12.2. Histology

Serial 7 μm-cross sections were obtained from the distal end of the regenerated nerve tissue and cut in proximal direction over a distance of approximately 1000 μm. Blind-coded sample sections (from $n = 5$ randomly chosen animals per group) taken from the distal end and 320 μm more proximal were processed in HE-staining in order to examine the number of multinucleated giant cells per mm^2 in the centre area as well as in the perineurium. Sections were examined in light microscopy (Olympus BX53; Denmark) software-aided with cellSense Dimensions (Olympus; Denmark). Overview photomicrographs were used for the measurements.

Additional blind-coded sample sections (from $n = 8$ randomly chosen animals per group) taken at defined distances in distal–proximal direction (0 μm (=1 mm in distal stump), 64 μm, 128 μm, 320 μm, 384 μm, 448 μm, 672 μm, 736 μm, 992 μm, 1056 μm (=distal end of former nerve defect)) were subjected to double-immunohistochemistry for activated macrophages (ED-1) and neurofilaments (NF-200). Blocking and ED-1-immunohistochemistry were performed as described above. After incubation with the secondary antibody the sections were further washed with PBS (3×) and a second blocking step with 0.5 M trisaline buffer (60.6 g tris + 9 g NaCl in 1.l H_2O; pH 7.4) containing 3% milk powder and 0.5% triton X-100 followed by overnight incubation (4 °C) with primary rabbit anti-NF-200 antibody (1:200; N4142, Sigma, Germany). After washing with trisaline buffer (3×), incubation with Alexa 488-conjugated secondary goat-anti rabbit antibody (1:1000, A11034, Invitrogen, Germany) was performed for 1 h at RT. Sections were finally counterstained with DAPI and mounted with Moviol. The nuclear DAPI counterstaining was used to clearly identify ED1-immunopositive cells but not for further quantification in this case.

For quantification of the number of activated ED1-immunopositive macrophages/mm^2, seven photomicrographs per section were randomly taken (20× magnification) in the outer area (4 photomicrographs) and in the centre area (3 photomicrographs) to examine approximately 32% of the complete section area. Finally, the thickness of the perineurium was evaluated on theses sections as well, therefore at three randomly chosen locations the thickness was determined and the mean calculated for each sample.

2.13. Analysis of tube properties after explantation

On day 5 and day 18 after nerve reconstruction the chitosan tubes were explanted. On day 18 a surrounding connective tissue could be dissected, macroscopically classified and processed for histological analysis. On day 5 and day 18 the tubes and their contents were stored for Western Blot analysis of the content. Therefore the middle parts of the tubes were harvested by cutting of the proximal and distal ends of the tubes at the suture sites. Also upon explantation in week 13 after nerve reconstruction (long term observation, 3 months), the tubes were explanted, dissected from surrounding connective tissue and stored in 0.9% NaCl solution for further analysis of biomaterial properties.

The properties of the tubes, the connective tissue as well as the macroscopic nerve cable peculiarities were then classified and connective tissue samples were processed for histological evaluation. Furthermore, tube samples (before and after nerve reconstruction) were analysed by Scanning electron microscopic (SEM) or biochemical tests ($n = 3$/group).

2.14. Statistics

In the different laboratories contributing to the presented study different statistical software was used, either the statistical package SPSS (version 17.0 or 20.0, IBM, USA) or GraphPad InStat software, version 5.0.3.0 & 6.00 for windows (Graphpad Software, CA, USA). A p value of <0.05 was taken as statistically significant. The statistical tests used for the different cytotoxical, functional and histological evaluations are stated in the respective results sections. For nerve stereology, the statistical analysis was performed using two or one-way ANOVA. If this analysis identified a significant difference the post-hoc HSD Tukey's test, or Bonferroni were applied for paired comparisons. Kruskal–Wallis, with subsequent Mann–Whitney as post-hoc, was used to detect differences between groups. Furthermore, the proportion of animals per group that displayed a predefined qualitative parameter (evocable CMAP) was calculated as percentage (0–100%) and analysed with the Chi-Square-test.

3. Results

3.1. In vitro cytotoxicity assays

In vitro cytotoxicity assays were performed to test the biocompatibility of the new chitosan tubes and the influence of the different degrees of acetylation (DA) on it. The MTS test revealed that the leachables and degradation products released by the chitosan tubes of different DA (i.e. DAI, DAII, DAIII) did not negatively affect the metabolic viability of RBMSCs when compared to the positive control (Fig. 3A). Similarly, the MEM extraction test revealed no negative influences on the cell densities (Fig. 3B). Therefore, the tested samples can be considered as non-cytotoxic, as the leachables and degradation products released by chitosan tubes tested with different DA did not induce any deleterious effects on RBMSCs.

3.2. In vivo evaluation after nerve reconstruction with chitosan tubes

Chitosan tubes of DAI, DAII, DAIII were implanted to bridge a 10 mm defect of lesioned sciatic nerves and compared with controls 5, 18, 21 days, and 3 months, respectively, after nerve reconstruction (Fig. 1).

3.2.1. Short term observation (5, 18 days)

Five and 18 days after nerve lesion and nerve reconstruction with chitosan tubes of different DAs, qRT-PCR for neurotrophic factors (NGF, FGF-2, BDNF), the cytokine IL-6, the BDNF-receptor TrkB and for GAP-43 were performed on DRGs (L3–L5). All data were normalized to the contralateral non-lesioned site of control animals in which the separated ipsilateral nerve ends were folded over and sutured to themselves. In accordance with the expression pattern in the DRGs of the control group, NGF, FGF-2, IL-6, BDNF and GAP-43 were up-regulated ($p \leq 0.05$, *t*-test) as well in the presence of the tubes, whereas TrkB remained unchanged in all experimental groups (Fig. 4A). In addition, there were no significant changes in the expression patterns of the respective neurotrophic factors between 5 and 18 days. It can be concluded that chitosan tubes do not influence the physiological up-regulation of neurotrophic factors following nerve injury.

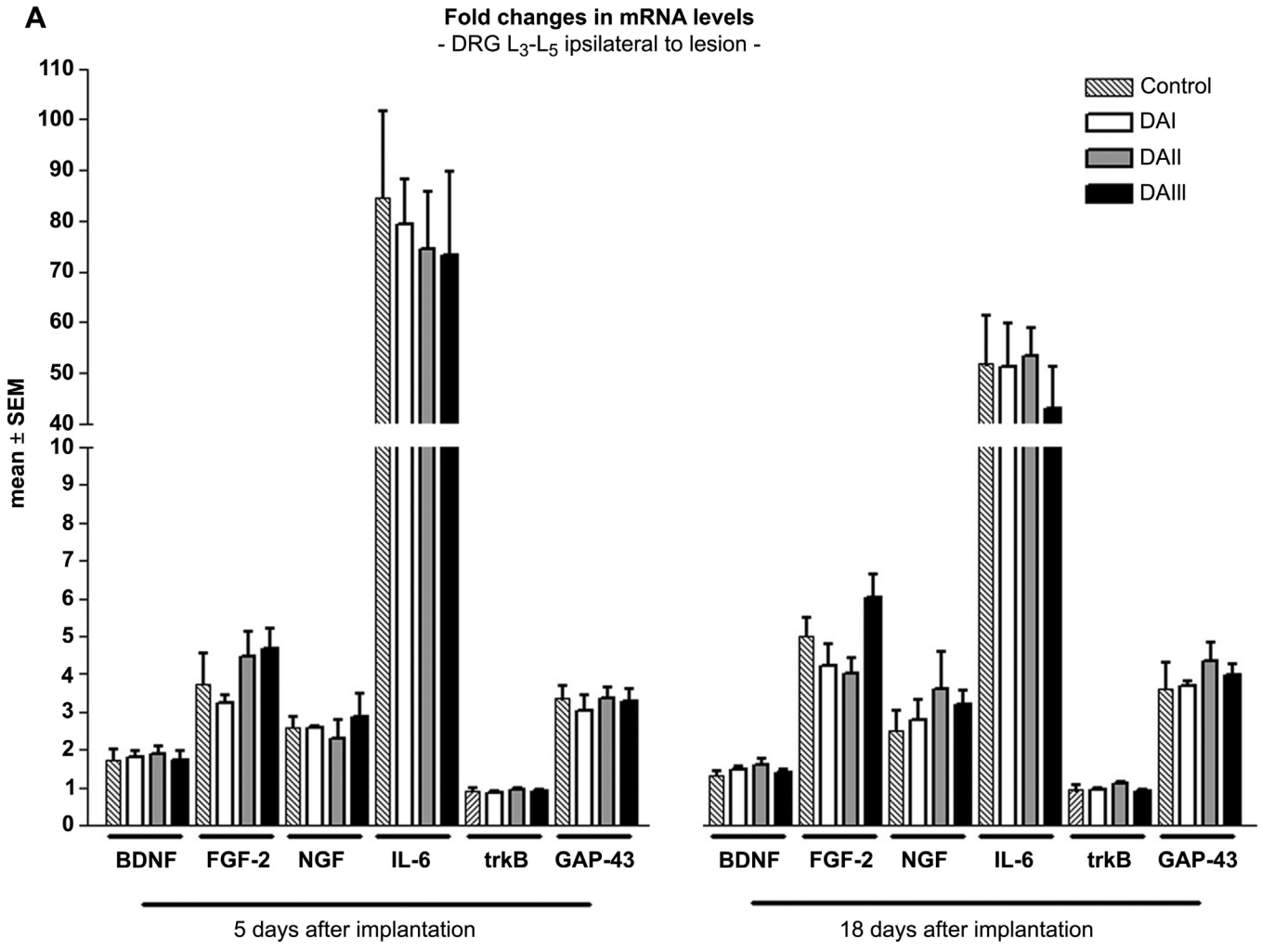

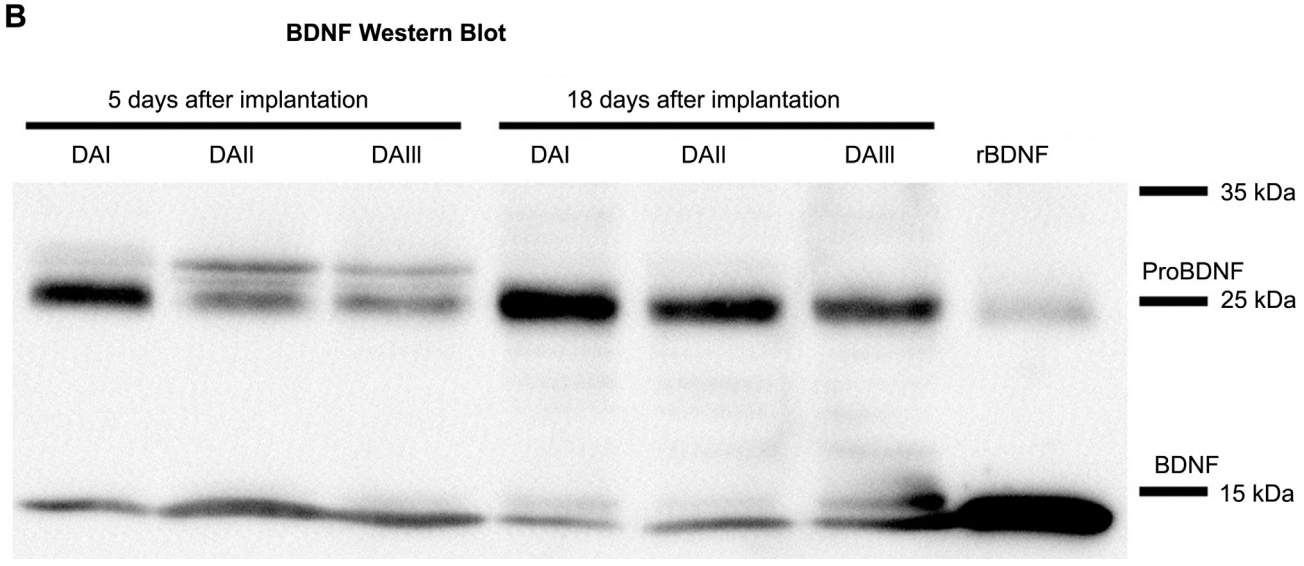

Fig. 4. (A) Regulation of mRNA levels of representative neurotrophic factors and regeneration associated proteins at the lesioned site, 5 and 18 days after nerve reconstruction with chitosan tubes or control surgery. Values were normalized to the non-lesioned site of the control group, DAI, DAII, DAIII, $n = 3$ each; control, $n = 4$. A representative Western Blot of pooled tube content ($n = 5–6$/group) is shown for BDNF (B). DAI = ~2%; DAII = ~5%; DAIII = ~20%.

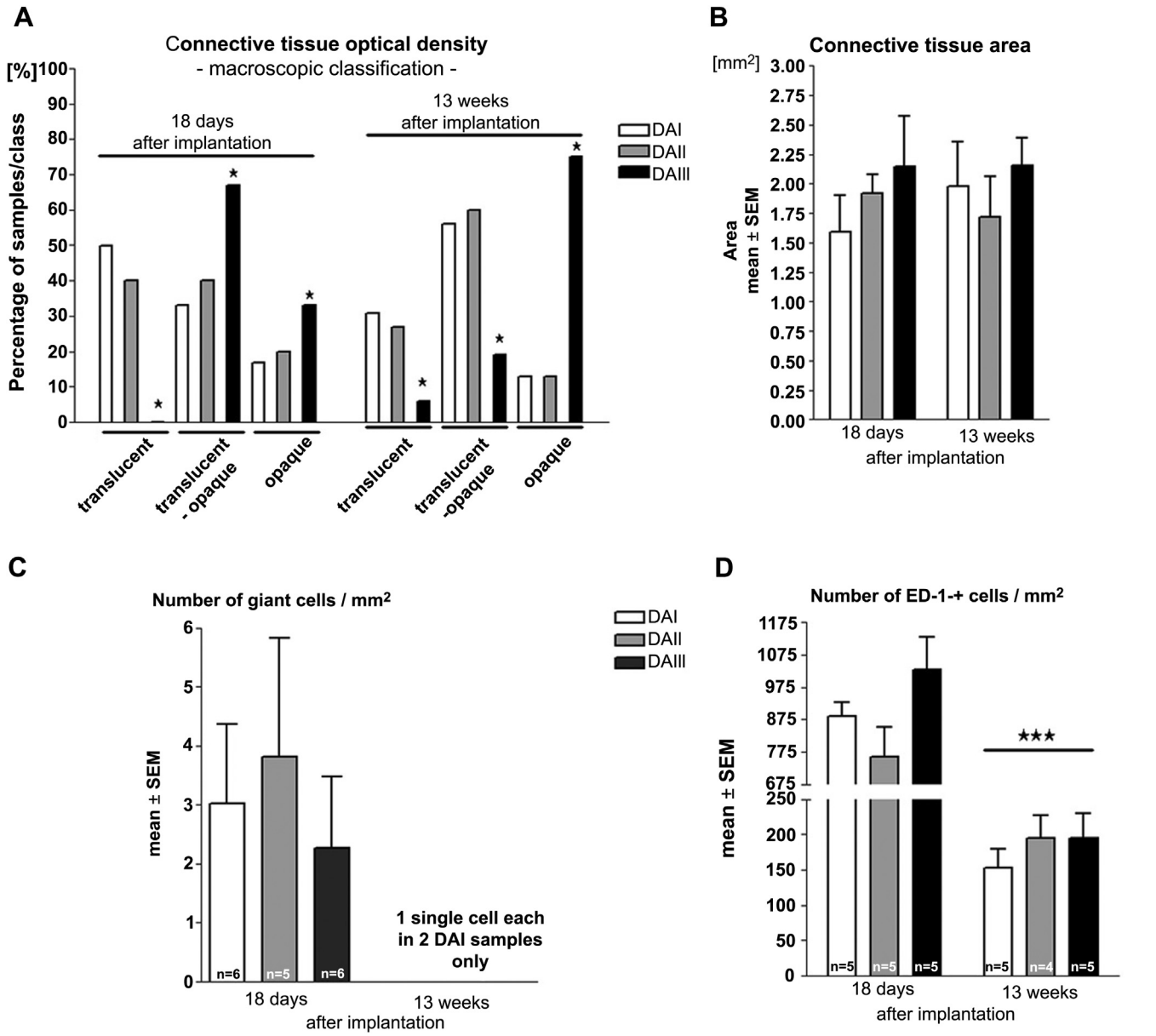

Fig. 5. Connective tissue developed around the chitosan tubes of different degree of acetylation was analysed for (A) its optical density and (B) its area [mm^2] as well as for (C) the number of multinucleated giant cells within the contact area to the chitosan tubes and (D) the number of activated macrophages (ED-1-immunopositive, ED1-+ cells). Significant changes were detectable between the short and the long term evaluation, but not among the connective tissue surrounding chitosan tubes of different degree of acetylation (DAI = ~2%; DAII = ~5%; DAIII = ~20%). Statistical tests used: (A) Chi-Square-test, asterix indicating differences between DAIII-tubes and others, $p < 0.05$; (C) Two way ANOVA, Tuckey's multiple comparison, asterix indicating difference to 18 days, $p < 0.001$.

Additionally, Western Blot analysis was performed from the tube content in order to detect the relative amounts of BDNF and NGF secreted into the chitosan tubes. Both, 5 and 18 days after nerve reconstruction pre-mature and mature BDNF and NGF (data not shown) were detectable in the pooled tube content with no difference between the DAs (Fig. 4B).

3.2.1.1. Connective tissue evaluation. Five days after nerve reconstruction with the chitosan tubes no surrounding connective tissue was detectable. At 18 days after nerve reconstruction, macroscopic evaluation revealed a significant shift to a higher optical tissue density for DAIII tubes (Fig. 5A). However, measurements of the connective tissue area (Fig. 5B) and thickness (data not shown) did not reveal any significant differences. The connective tissue contact area with the implanted tubes was further examined on HE-stained sections with regard to the presence of multinucleated giant cells and on ED1-immunopositive/DAPI counterstained sections with regard to activated macrophages, respectively. The quantification of giant cells, which are typically found in the environment of foreign materials, revealed no differences among the connective tissue in contact with DAI, DAII or DAIII chitosan tubes (Fig. 5C). Also the number of activated macrophages (ED1-immunopositive cells) was not altered among the different DAs (Fig. 5D).

3.2.2. Nerve regeneration, activation and apoptosis in short term (21 days)

3.2.2.1. The formed matrix. A matrix was formed in the chitosan tubes at 21 days. In separate experiments (results not shown), the content of the tube was examined at 10, 14 and 18 days, but there was not a sufficient and bridging matrix formed at these time

points. The thickness of the matrix in the different tubes was measured at three different sites (Fig. 6A; Table 1), and showed a somewhat hourglass shape, and with no statistical differences between the three types of acetylation tubes at any of the measured sites (Table 1).

3.2.2.2. Axonal outgrowth and Schwann cells. The immunohistochemical evaluation revealed a length of axonal outgrowth of about 7.9–8.6 mm in the three acetylation variants with no statistical difference present (Kruskal–Wallis $p = 0.28$), but with a tendency to shorter growth in the DAIII-tube group. S-100 staining revealed that Schwann cells were present in the matrix along the entire tube (Fig. 6B).

3.2.2.3. ATF3 stained Schwann cells. Few ATF3 stained cells were present in the matrix, but without any significant difference (Table 1) in the tubes, although DAPI stained cells were seen. However, a considerable number of ATF3 stained cells, with a significant difference between the three DAs (i.e. lowest in DAI- and highest in DAIII-tubes), was present in the distal nerve segment at 21 days (Table 1).

3.2.2.4. Cleaved caspase 3 stained Schwann cells. In contrast to ATF3 staining, cleaved caspase 3 stained cells were observed in the matrix along the entire length of the matrix in all three types of the chitosan tubes (Table 1, Fig. 6B). Significantly increasing higher cell numbers were detected in the formed matrix with increasing degree of acetylation of the tubes; i.e. with a low number in DAI tubes. There were extensive numbers of cleaved caspase 3 stained Schwann cells in the distal nerve segment, but with no difference between the tubes of different DAs.

3.2.2.5. Total number of DAPI-stained cells. DAPI-stained cells were present in the matrix of all tubes, but with no difference among the DAs. However, there was a significant difference in DAPI-stained cells in the distal nerve segment (Table 1).

3.2.2.6. Correlations. The thickness of the formed matrix correlated strongly with the length of the axonal outgrowth (rho-value up to 0.9; p-value < 0.02; Spearman), particularly in the DAI- (~2%) and DAIII- (~20%) tubes. The length of axonal outgrowth did only correlate with the number of cleaved caspase 3 stained Schwann cells in the distal nerve segment (rho 0.44, $p = 0.016$).

In the distal nerve segment, the number of cleaved caspase 3 stained Schwann cells negatively correlated (rho −0.53, $p = 0.003$) with the total number of DAPI stained cells, particularly in DAIII-tubes. No other relevant correlations were observed.

3.2.3. Long term observation (13 weeks) regeneration

3.2.3.1. Functional recovery. Long term regeneration was evaluated with regard to functional recovery analysing the SSI and non-invasive and invasive electrophysiology after different time points

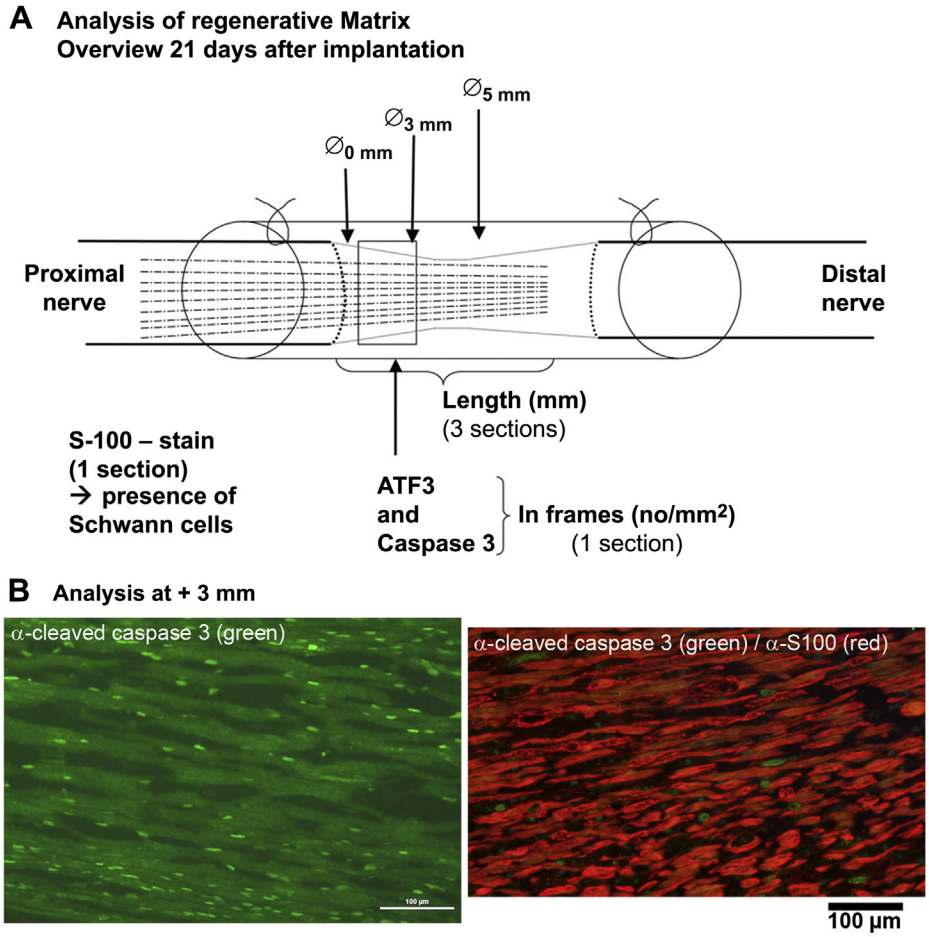

Fig. 6. (A) Overview of the quantification of matrix, axonal outgrowth, activated and apoptotic Schwann cells and total number of cells (DAPI) in the model. (B) Representative photomicrographs taken at +3 mm within the matrix in sections incubated with α-cleaved caspase 3 antibody (green, apoptotic cells; left panel) and α-S100 antibody (red, Schwann cells; double staining, right panel).

Table 1
Dimensions, length of axonal outgrowth, and numbers of activated and apoptotic Schwann cells and total number of DAPI stained cells in the matrix and in the distal nerve segments in rat sciatic nerve defects bridged by differentially acetylated chitosan tubes (DAI = ~2%; DAII = ~5%; DAIII = ~20%).

	DAI ($n = 10$)	DAII ($n = 10$)	DAIII ($n = 9$)	p-Values
Matrix diameter at 0 mm (μm)	317 [303–339]	313 [303–334]	303 [292–321]	0.36
Matrix diameter at 3 mm (μm)	242 [222–302]	250 [236–287]	232 [224–245]	0.29
Matrix diameter at 5 mm (μm)	242 [232–278]	248 [232–280]	237 [228–244]	0.54
Axonal outgrowth (mm)	8.61 [7.51–9.01]	8.64 [8.04–9.31]	7.91 [7.43–8.76]	0.28
ATF3 stained cells in the matrix (at 3 mm) (% of total)	0.4 [0–0.7]	0.4 [0–0.7]	0.3 [0–0.3]	0.39
ATF 3 stained cells in the distal nerve segment (% of total)	19.8 [18.6–21.6][c]	25.2 [20.2–28.3][b]	30.6 [27.9–35.3]	**0.0001**
Cleaved caspase 3 stained cells in the matrix (at 3 mm) (% of total)	4.7 [2.7–7.6][a]	15.3 [5.8–19.5][b]	20.5 [18.0–23.0]	**0.0001**
Cleaved caspase 3 stained cells in the distal nerve segment (% of total)	22.1 [20.5–28.3]	27.7 [22.9–34.9]	21.5 [20.4–22.9]	0.07
Total number of DAPI stained cells in the matrix (no/mm^2)	1010 [966–1046]	1057 [981–1080]	1011 [833–1030]	0.18
Total number of DAPI stained cells in the distal nerve segment (no/mm^2)	981 [914–1022][a]	888 [866–919][b]	1094 [1059–1142]	**0.0001**

Values are median [25th–75th percentiles]. p-Values based on Kruskal–Wallis-test.
Bold writing indicates statistical significance.
[a] Different from medium and high acetylation.
[b] Different from high acetylation.
[c] Different from high acetylation (Mann–Whitney-test).

(Fig. 1). Eventual changes from initial numbers of animals per group are indicated throughout and due to hamstring toe contractures or signs of autotomy, which excluded animals from certain tests at a certain time point. Additionally, few animals died over the long term observation period because of low tolerance to the repeated anaesthesia. Actual animal numbers are appropriately indicated in the graphs below.

3.2.3.2. Static sciatic index (SSI). With regard to the SSI a significant decrease from pre to post nerve defect and reconstruction was found which remained significantly decreased till the end of the observation period. Interestingly, the post-surgery performances of the different experimental groups revealed no significant differences, also when comparing the reconstruction of the nerve with hollow chitosan tubes to the autologous nerve graft (Fig. 7A). This suggests that the hollow chitosan tubes, independently of their DA, influence motor regeneration in the same extent as the gold standard.

3.2.3.3. Electrophysiological assessment. Compound muscle action potentials (CMAPs) were serially recorded from the tibialis anterior muscle (TA) and plantar muscles (PL) at 4, 9, and 12 weeks after nerve reconstruction. Additionally, a final invasive recording was performed on the last day of observation in week 13. Four weeks after nerve reconstruction no CMAPs were evocable for both locations. However, nine weeks after nerve reconstruction 62% of the animals treated with autologous nerve grafts demonstrated evoked CMAPs in the TA, while significantly less animals of the other groups showed these signs of reinnervation (6–29%, Table 2). Twelve weeks after nerve reconstruction the number of chitosan tubes treated animals with evoked CMAPs recordable from the TA muscle reached a level comparable to the autologous nerve grafted animals. When recordings were performed from the PL muscles, a similar development of motor recovery was detectable (Table 2). These data reveal that chitosan tubes of all degrees of acetylation allow functional recovery, which almost reaches the same distribution as after autologous nerve grafting.

Furthermore, the CMAPs were analysed in more detail, as was the nerve conduction velocity (NCV). No significant differences among the amplitudes of evocable CMAPs could be detected among the groups during the non-invasive and invasive measurements (data not shown). Also for the NCV-ratio (ipsilateral/contralateral), the TA and the PL muscles data revealed no significant differences in comparison with autologous nerve grafting and bridging of the nerve defects with chitosan hollow tubes or among the chitosan tubes with different degrees of acetylation (Fig. 7B).

3.2.3.4. Muscle weight ratio. After the final electrophysiological measurements, the muscle weight ratios (g_{ipsi}/g_{contra}) of the lower limb muscles were determined after harvest of the tibialis anterior and gastrocnemius muscles (Fig. 1) and revealed no differences among the experimental groups (Fig. 7C).

3.2.4. Histomorphological evaluation

3.2.4.1. Distal nerve stereology. The results of the stereological assessment of myelinated fibre number and axon diameter, fibre diameter, myelin thickness and g-ratio of all experimental groups are shown in Fig. 8. The total numbers of myelinated fibres (Fig. 8A) are significantly different in all groups towards the healthy nerve ($^{*}p \leq 0.05$; $^{**}p \leq 0.01$), but only the nerve distal to DAI-chitosan tubes is significantly different compared to the autologous nerve graft group ($\#p \leq 0.05$). With regard to axon and fibre diameters and myelin thickness (Fig. 8B), all the experimental groups differ from healthy nerves ($^{**}p \leq 0.01$) but no differences are seen among them. In Fig. 9 high-resolution representative images of semithin sections of regenerated sciatic nerves are shown in comparison to the contralateral healthy control (Fig. 9A: healthy contralateral nerve; Fig. 9B: autologous nerve graft; Fig. 9C: DAI; Fig. 9D: DAII; Fig. 9E: DAIII). Nerve fibre size distribution is also reported (Fig. 9F–J). The distribution is significantly different between healthy and regenerated nerves but again no significant differences in fibre size distribution could be detected among the experimental groups.

3.2.4.2. Immunological nerve tissue reaction. In addition to the stereology, the area around the distal suture (bridging 1 mm distance, see Fig. 1) was evaluated with regard to the presence of activated macrophages in the regenerated nerve tissue after double-staining for the ED1-antigen and NF200-Neurofilaments (Fig. 10A–C). Whereas in nerves regenerated through DAI and DAII chitosan tubes similar amounts of ED1-immunopositive cells were found, nerves regenerated through DAIII chitosan tubes contained significantly higher numbers of these cells, i.e. activated macrophages. As expected, in all tubes the number of macrophages was significantly lower than in autologous nerve grafts where it can be attributed to myelin debris removal (Fig. 10D). On the same sections of the regenerated nerves the thickness of the perineurium was measured. Interestingly, whereas thickness of the perineurium of nerves regenerated through DAI and DAII chitosan tubes was comparable with the perineurium thickness in the autologous nerve graft group, nerves regenerated through DAIII chitosan tubes displayed a significantly thicker perineurium (Fig. 10E). The higher number of macrophages together with a thicker perineurium point to an immunological reaction in DAIII.

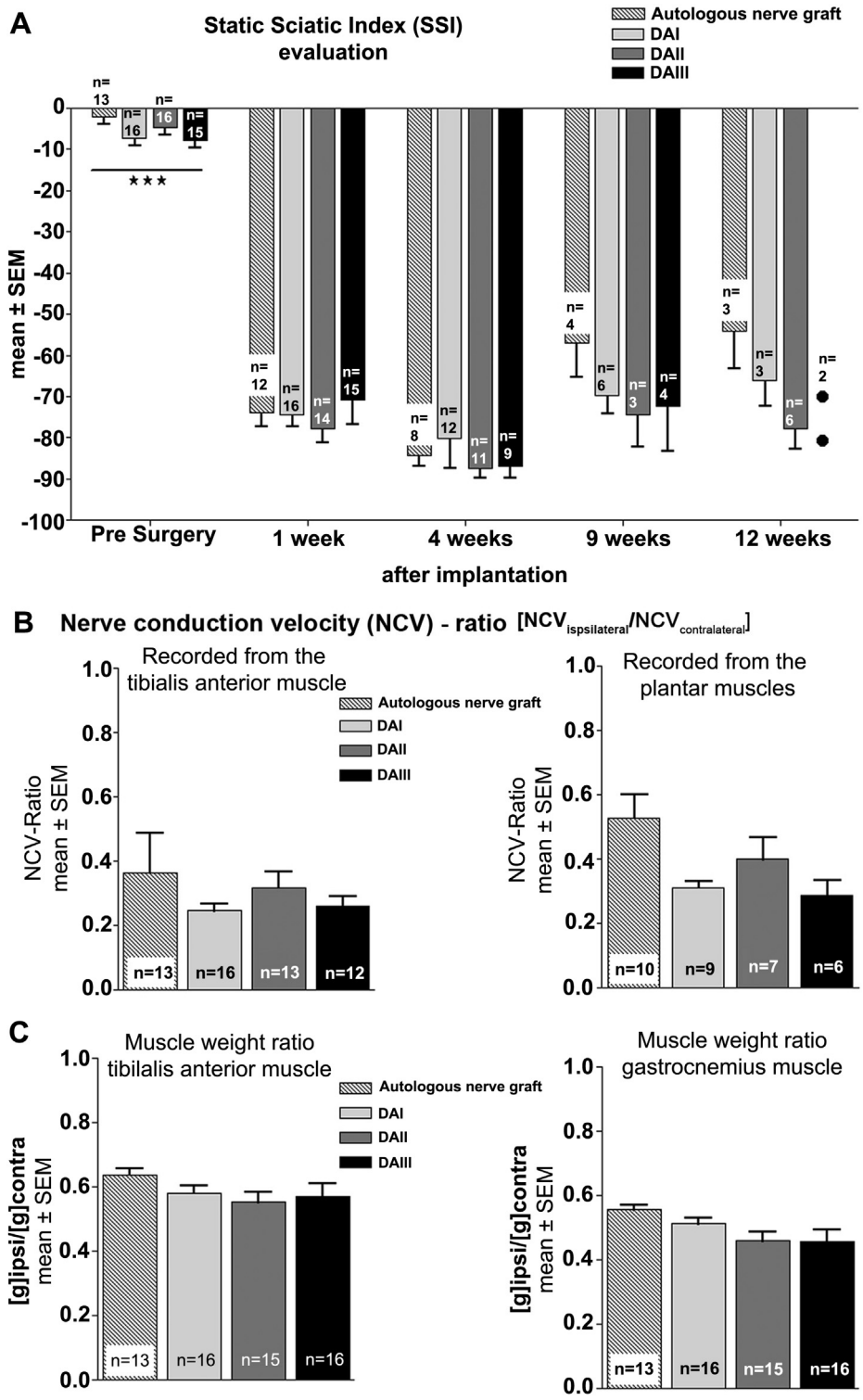

Fig. 7. Functional evaluation of motor recovery revealed no significant differences among the gold standard autologous nerve graft and the nerve reconstruction with chitosan tubes of different degree of acetylation. DAI = ~2%; DAII = ~5%; DAIII = ~20%. (A) Results of the calculation of the static sciatic index (SSI). Statistical test: two way ANOVA, Tukey's multiple comparison, triple asterix indicating difference to post nerve lesion values, $p < 0.001$. (B) Calculation of the nerve conduction velocity ratio. (C) Calculation of the lower limb muscle weight ratio.

3.2.4.3. Connective tissue evaluation. There was never a strong scar tissue formation around the chitosan tubes. Similar as performed 18 days after nerve reconstruction (Fig. 1), the connective tissue surrounding the tubes was explanted and analysed morphologically with regard to its optical density, its area and thickness, the presence of multinucleated giant cells (HE staining, Fig. 2B), and immunohistochemically for the presence of activated macrophages (ED1-immunopositive cells). Similar to the findings after short term nerve reconstruction, the optical density of the connective tissue surrounding DAIII chitosan tubes was significantly increased in

Table 2
Increasing distribution of animals per group which showed evocable compound muscle action potentials in the tibialis anterior or plantar muscles during the regeneration period after autologous nerve grafting or nerve reconstruction with chitosan tubes of different degree of acetylation (DAI = ~2%; DAII = ~5%; DAIII = ~20%).

	9 weeks			12 weeks			13 weeks (invasive)		
	Animals/group	Percentage	Significant difference	Animals/group	Percentage	Significant difference	Animals/group	Percentage	Significant difference
Tibialis anterior muscle									
Autologous nerve graft	8/13	62%		13/13	100%		13/13	100%	
DAI	1/17	6%	#	14/16	88%	#‡	16/16	100%	‡
DAII	2/16	13%	#	11/16	69%	#†	13/14	93%	#†
DAIII	5/17	29%	#†‡	13/16	82%	#†	12/15	80%	#†‡
Plantar muscles									
Autologous nerve graft	8/10	80%		10/10	100%		10/10	100%	
DAI	5/10	50%	#	8/10	80%	#‡	9/10	90%	#‡
DAII	6/12	50%	#	7/11	64%	#†	7/10	70%	#†
DAIII	4/12	33%	#†	7/11	64%	#‡	6/9	67%	#†‡

Significant differences $p < 0.05$ are indicated as follows: # versus nerve autograft, † versus DAI-chitosan tube, ‡ versus DAII-chitosan tube.

comparison to the connective tissue from the other groups (Fig. 5A). Connective tissue area and thickness displayed no significant differences among chitosan tubes of different DAs after 3 months and, in addition, no significant differences were obvious when compared with the data after 18 days (Fig. 5B). Multinucleated giant cells were only detected in two animals (DAI group) displaying a significant reduction of the foreign body reaction at 3 months after nerve reconstruction (Fig. 5C). Quantification of ED1-immunopositive cells revealed a highly significant reduction of their appearance as compared to the evaluation after short term nerve reconstruction (18 days, Fig. 5D). However, at both time points no differences in the immunological connective tissue reaction to chitosan tubes of different degrees of acetylation were obvious.

3.2.5. Assessment of chitosan tube properties after explantation

In addition to the above mentioned analyses of the connective tissue and regenerated nerve tissue peculiarities, the chitosan tubes were also macroscopically analysed upon explantation. The properties of the tubes differed substantially among the different degrees of acetylation. While 5 days after nerve reconstruction no macroscopic differences were detectable, DAIII-chitosan tubes showed signs of beginning degradation already 18 days after nerve reconstruction. In two of six DAIII-tubes small longitudinal fissures were visible through the surgery microscope and a 3rd sample displayed a rough surface. The degradation of DAIII-chitosan tubes was much further in progress three months after nerve reconstruction when these tubes displayed longitudinal fissures (4 out of 15), a fragmentary appearance that broke apart upon nerve tissue harvest (8/15) or they were already longitudinally broken and compressed (3/15). The crack-lines and sharp edged pieces appearing with progressed degeneration could have potentially damaged already regenerated nerve tissue. In contrast, DAI- and DAII-chitosan tubes mostly displayed a regular shape and firmness (13/16 and 11/15, respectively) and rarely a slightly bent shape (3 each) or a slight compression (DAII only: 1/15), both together with regular firmness. The colour of DAI and DAII tubes was changed to a serous yellow, while in DAIII tubes the change of colour was minimal. Fig. 11 shows representative samples of all chitosan tube types before and after nerve reconstruction. A cracked DAIII-chitosan tube 13 weeks after nerve reconstruction is shown in Fig. 12, demonstrating that degeneration of the tubes leads to damages that are already microscopically evident and can easily be confirmed in ultrastructural images.

Table 3
Results of the mechanical and biochemical analyses of chitosan tubes, which were explanted 13 weeks after nerve reconstruction. The degree of acetylation was determined in NMR spectrometry and the molecular weight (MW) was determined using the GPC method. With the latter no clear differences have been detected among the chitosan tubes of different DA. The symbols shown in the respective column show a tendency to most obvious reduction of MW in DAI chitosan tubes.

Chitosan tubes	Before implantation DA	13 weeks after nerve reconstruction			
		DA	Solubility	Toughness	MW degradation
DAI	~2%	1.1% ± 0.3%	−−	++	+++
DAII	~5%	3.6% ± 0.3%	−	+	++
DAIII	~20%	14.6% ± 1.1%	++	−− (brittle)	+

3.2.5.1. Biochemical characterization (Table 3).

The GPC chromatographs obtained showed an increase in the retention time for all chitosan tubes (the molecular weight distribution has shifted to the right) independently of the DA of the raw material. This evidence highlights the fact that all chitosan tubes used to bridge the nerve defects suffer depolymerisation during the time in vivo after nerve reconstruction. The DAIII-tubes showed a more symmetrical molecular weight (MW) degradation when compared with the other chitosan tubes with less DA. Nevertheless all samples analysed from the same group of chitosan tubes (DAI, DAII or DAIII) showed a similar chromatographic profile among them. This demonstrates a rather high reproducibility of the MW of the biopolymer (dispersibility of molecular weights) within the sample tubes, which suggests that both the tube production and biological activity are similar for each group. Homogeneity of the results within the three groups DAI–DAIII was quite high.

The variation of the DA among the chitosan tubes prior to nerve reconstruction and after explantation at 3 months was also investigated. Upon analytical evaluation of the NMR spectra, all sample chitosan tubes showed a rather similar DA before and after nerve reconstruction, demonstrating that there is no visible hydrolysis of the remaining acetyl groups of the chitosan main chain by biological action. Regarding solubility there was a clear tendency of chitosan tubes with higher DA to show a higher solubility when compared with other chitosan tubes of lower DA. In the case of DAI-chitosan tubes (DA ~2%) it was necessary to heat the solution in order to achieve a total dissolution of the tubes. On the other hand, the toughness of the tubes after explantation at 3 months was higher in DAI and DAII chitosan tubes when compared to DAIII-tubes, which were brittle.

4. Discussion

During the last years there has been an interest in chitosan as a suitable biomaterial for medical and pharmaceutical applications

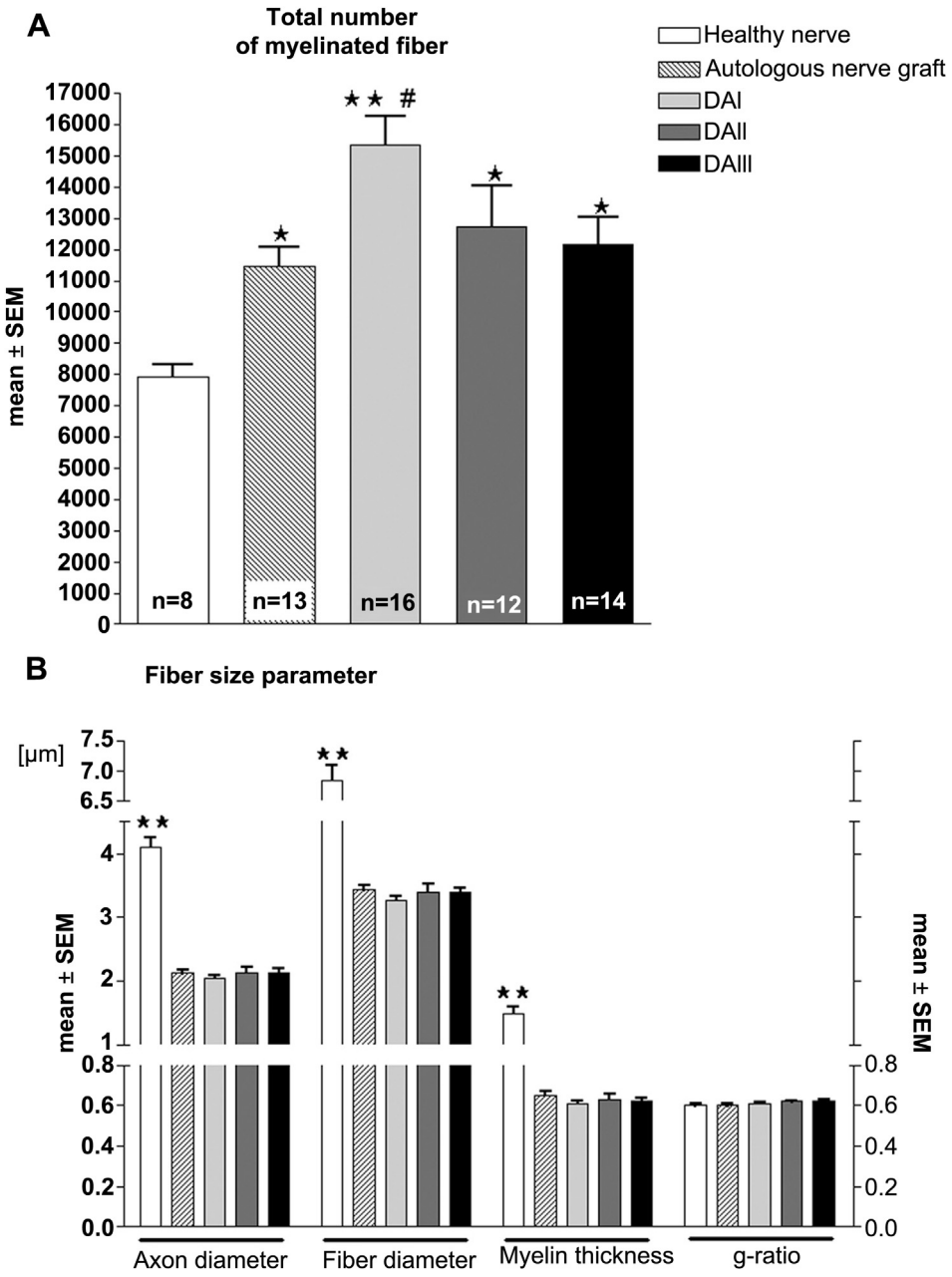

Fig. 8. The distal nerve (5 mm segment harvested 1 mm distal to the distal suture) was stereologically analysed in order to assess the myelinated fibres. (A) Result of myelinated fibre quantification. (B) Results of fibre size parameter analyses. Samples of healthy contralateral nerves were compared to nerve samples regenerated through autologous nerve grafts or chitosan tubes of different degrees of acetylation (DAI = ~2%; DAII = ~5%; DAIII = ~20%). $^{*}p \leq 0.05$ and $^{**}p \leq 0.01$: experimental groups vs healthy nerve; $\#p \leq 0.05$: DAI vs autologous nerve graft.

because of its biocompatibility, non-toxicity, and biodegradability. These properties qualified chitosan also as a putative candidate material for fabrication of peripheral nerve reconstruction devices [18,32]. However, the poor mechanical strength of chitosan conduits, along with pre-mature degradation and loss of structural integrity in vivo, were major limitations which prevented their commercial application in neural tissue engineering until now [15,18,32]. The present study, using chitosan conduits with different degrees of acetylation, indicates that fine-tuned chitosan tubes induce sufficient peripheral nerve regeneration when used to reconstruct a 10 mm nerve defect in adult rat sciatic nerves.

In vitro cytotoxicity tests with extracts from the different chitosan tubes revealed no detrimental effects on cell metabolic viability. Indeed when observing Fig. 3, it is noticeable that the values obtained are even above those obtained with the positive control extracts. As it is known chitosan withholds several structural affinities with animal/human tissues [33], however, when it degrades it can induce an increase of cell metabolic viability. Moreover, this is probably the reason why DAIII extracts disclose higher metabolic viabilities when compared to DAI or DAII extracts.

Short and long term in vivo studies demonstrated that i) mainly DAII chitosan tubes support nerve regeneration in a similar extent as the gold standard autologous nerve graft with regard to both function and morphology, while DAI and DAIII chitosan tubes demonstrated some shortcomings ii) the lesion-induced regulation of regeneration associated neurotrophic factors in the corresponding dorsal root ganglia and the secretion of BDNF and NGF into the chitosan tubes was not altered due to their different DAs,

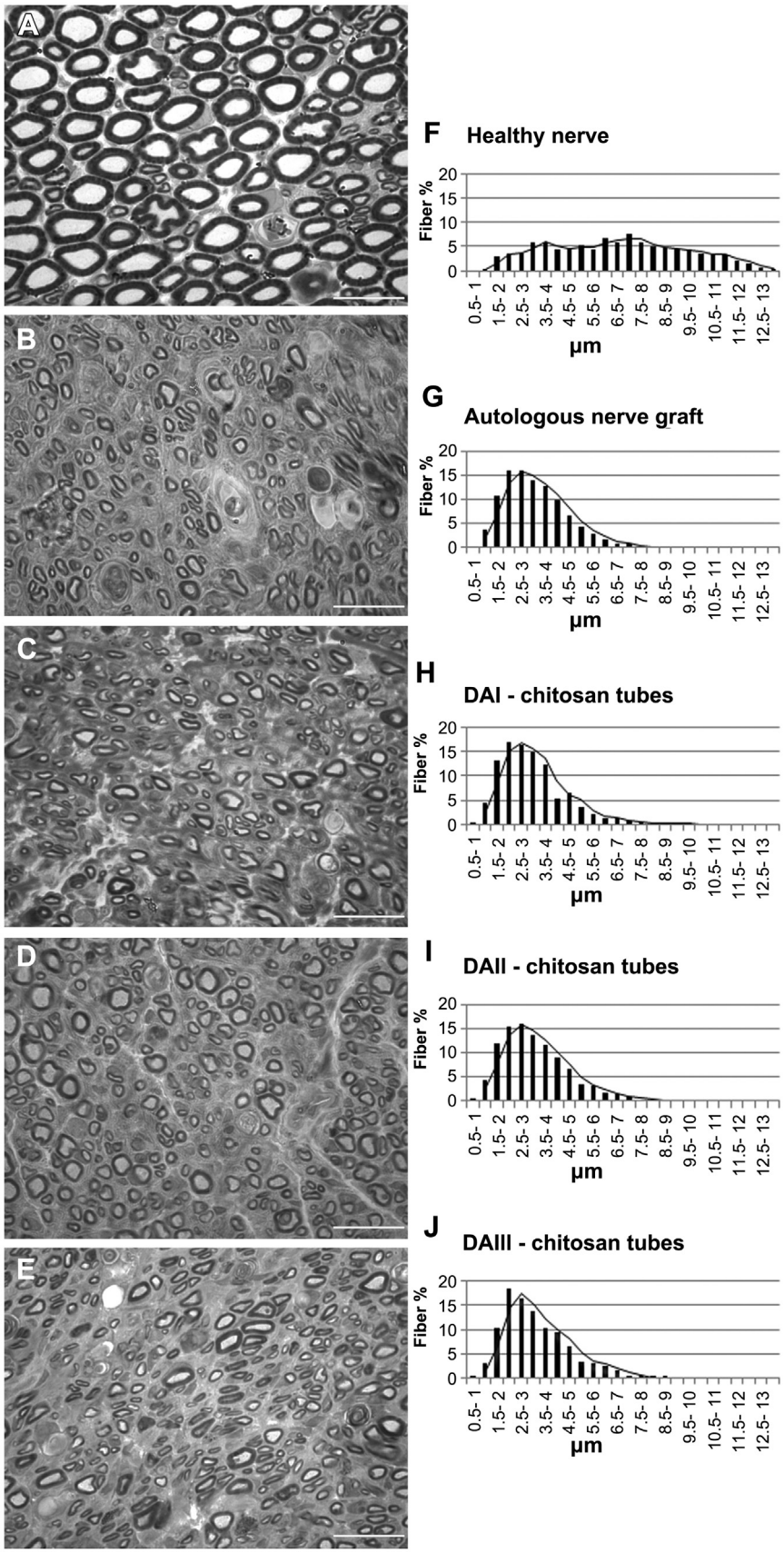

Fig. 9. High resolution images of representative semithin sections, stained with Toluidine blue, of nerve samples (A) from a healthy contralateral nerve, (B) regenerated through an autologous nerve graft, (C)–(E) regenerated through chitosan tubes (DAI = ~2%; DAII = ~5%; DAIII = ~20%). Scale bars: 20 µm. (F)–(J) fibre size distribution in the analysed groups of nerve samples.

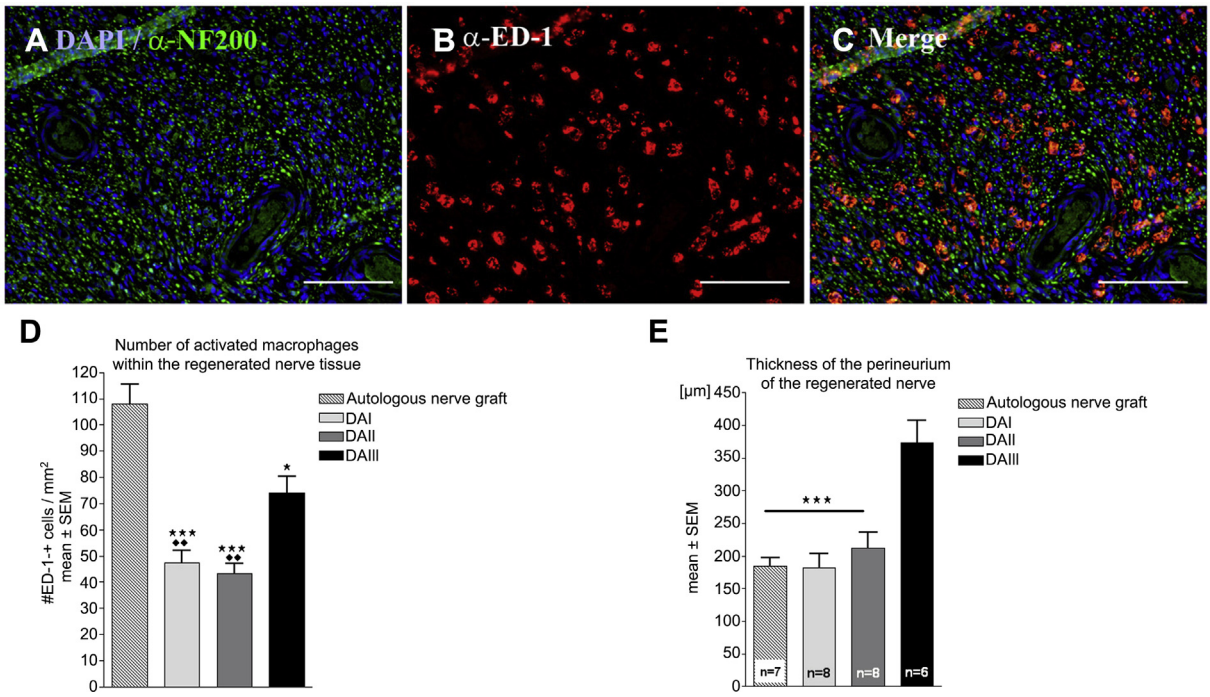

Fig. 10. (A)–(C) Representative photomicrographs of a cross-section of nerve tissue regenerated through DAIII-chitosan tubes analysed for the number of activated macrophages (ED-1-immunopositive cells), Scale bars: 100 µm. (D) Results of ED-1-cell quantification. Significantly less immunological tissue reaction was seen in nerves regenerated through DAI- or DAII-chitosan tubes compared to DAIII-group samples. (E) Measurement of the thickness of the perineurium in the regenerated nerve tissue further revealed that significantly more connective nerve tissue was formed inside of DAIII-chitosan tubes when compared to DAI- and DAII-tubes. DAI = ~2%; DAII = ~5%; DAIII = ~20%. Statistical tests used: (D) Kruskal–Wallis Test, Dunn's multiple comparison, asterix indicating inter-group differences to autologous nerve graft and solid rhombus indicating inter-group difference to DAIII-chitosan tubes $p < 0.05$; (E) One way ANOVA, Bonferroni multiple comparisons test, asterix indicating difference to DAIII-chitosan tubes, $p < 0.001$.

iii) the regenerative matrix formed in DAI and DAII chitosan tubes contained a lower number of cleaved caspase 3 stained, i.e. apoptotic, Schwann cells, as compared to DAIII chitosan tubes, iv) the number of ED1-immunopositive cells, i.e. activated macrophages, and thus the tissue reaction, in the regenerated nerve was significantly lower after nerve reconstruction with DAI and DAII chitosan tubes, and v) the material-induced immunoreaction in the connective tissue formed around the chitosan tubes was not altered by their different DA (equal numbers of multinucleated giant cells and activated macrophages) and was considerably reduced from 18 days to 3 months after nerve reconstruction.

Although the chitosan tubes with the different DAs allowed good structural and functional sciatic nerve regeneration, there were obvious differences with regard to the speed of their degradation (structural integrity), which were most evident at 3 months after nerve reconstruction. Overall, the DAIII chitosan tubes were much less stable during the observation period, which is probably the reason for the development of connective tissue with a significantly higher optical density. After explantation, tubes of the different DAs revealed differences with regard to consistency and chemical properties, which were related to the different grades of degradation. Macroscopically detectable crack lines were also obvious in SEM ultrastructures, although the electron microscopic appearance was rather similar among the three groups. However, the DAI chitosan tubes display almost no degradability.

Regarding previous chitosan devices, the main differences to the chitosan tubes presented here include their fine-tuned chemical structure which provided an optimal substrate for the formation of a regenerative matrix, where the thickness of such matrix correlated to the length of the outgrowing axons in accordance with findings from silicone tubes [34]. This goes along with the high mechanical compression strength and collapse stability. Furthermore, these chitosan tubes are completely transparent to ease the surgical procedure, and because also microneedles go through the material very easily, they seemed to be very suitable for bridging nerve defects. Moreover, the chitosan raw material and the tubes are manufactured according to ISO standard protocols for medical devices, which is a pre-requisite for regulatory approval and commercial application.

Analysis of the early regeneration phase (21 days) after nerve reconstruction with the chitosan tubes of different DAs demonstrated a higher number of activated Schwann cells in the distal segments of nerves regenerated through DAIII tubes. This may mirror that Schwann cells are stimulated and prepared to attract the outgrowing axons [26,27]. However, there was a tendency to shorter axonal outgrowth in this early regeneration phase in the same group of animals. In addition, the number of cells stained for cleaved caspase 3 was significantly higher in the regenerative matrix within DAIII chitosan tubes. The latter may be detrimental for axonal outgrowth although the number of such cells did not correlate with axonal outgrowth.

While usually not considered in studies where new materials are analysed, it is worth to consider other endogenous early events of regeneration in addition to the immunological reaction and the regenerative efficiency in the presence of the foreign material. During regeneration a distinct pattern of neurotrophic factors is produced and secreted by the nerve ends [35]. Pooled tube contents were collected at 5 and 18 days after nerve reconstruction and Western Blots were performed for BDNF and NGF, which revealed no differences among the different experimental groups. Moreover, the analysis of the corresponding dorsal root ganglia for expression of different growth factors, which are regulated during the regeneration process, did also not reveal differences among the different experimental groups. This suggests that the presence of the chitosan tubes, irrespective of their DAs, does not disturb these molecular processes.

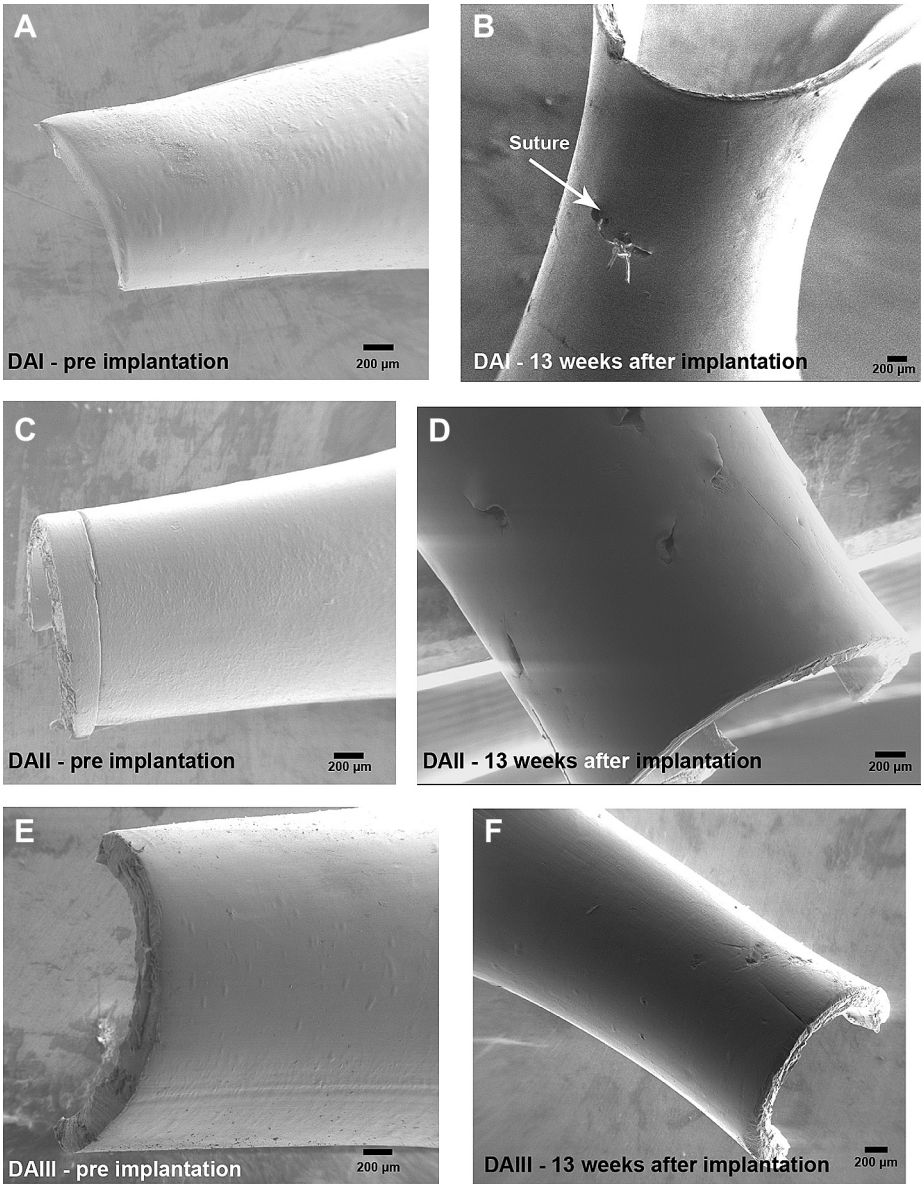

Fig. 11. Left column: representative SEM images of chitosan tubes of different degree of acetylation before nerve reconstruction. Right column: representative SEM images of example chitosan tubes explanted and analysed 13 weeks after nerve reconstruction. DAI = ~2%; DAII = ~5%; DAIII = ~20%.

Up to now the nerve reconstruction with an autologous nerve graft is the gold standard to overcome substance loss after peripheral nerve injury [1]. Thus, any nerve conduits have to be compared with this standard. With regard to the stereological parameters of the regeneration efficiency, the chitosan tubes presented in this study supported axonal regrowth to a similar extent as the autologous nerve graft. However, nerves regenerated through DAI chitosan tubes revealed a significantly higher total

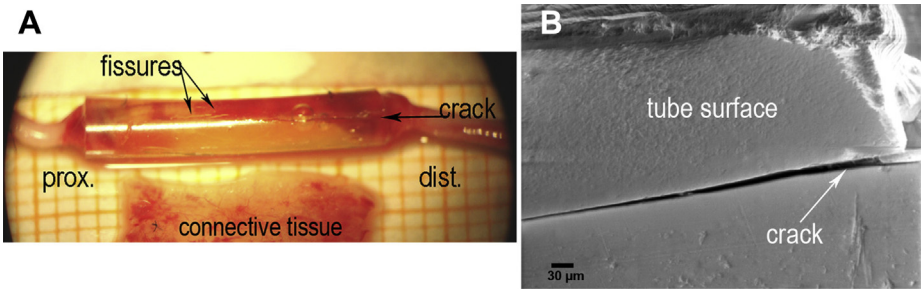

Fig. 12. (A) Chitosan tube of DAIII (~20% acetylation) upon explantation 13 weeks after nerve reconstruction, displaying several longitudinal fissures and a clear crack line. The connective tissue is opaque and the tube contains regenerated nerve tissue. (B) SEM image displaying the ultrastructure of the DAIII chitosan tube shown in (A) as well as the roughened outer surface of the tube after long term in vivo.

number of myelinated axons as compared to the gold standard. The increased number of regenerated axons after 3 months can be the morphological correlate of enhanced sprouting in the presence of DAI chitosan tubes, although fibre size under all experimental conditions was not different. Enhanced sprouting could eventually become a limiting factor for the outcome of functional recovery [36] and thus argues against the use of DAI chitosan tubes for future trials.

The good morphological regeneration in the presence of chitosan tubes is also reflected in the behavioural and functional parameters analysed. Regarding the SSI, animals of the different experimental groups displayed no significant differences compared to the gold standard. Moreover, although the electrophysiological measurements revealed a faster functional recovery in animals treated with autologous nerve grafts, after 3 months there were no significant differences with regard to the functional data among all experimental groups detectable. Interestingly, we found morphological differences with regard to non-neuronal tissue in the regenerated nerves, which have important impact on the selection of the type of chitosan tube for future applications. Three months after nerve reconstruction, the highest number of activated macrophages was present in nerves regenerated through autologous nerve grafts, which is due to the need for myelin debris removal in the autografts [35]. However, it is noteworthy that the number of activated macrophages within the regenerated nerves was significantly increased in the DAIII samples when compared to DAI and DAII samples. In addition, the thickness of the perineurium was significantly higher in nerves regenerated through DAIII chitosan tubes compared to DAI and DAII tubes and the autologous nerve graft. Both facts could reflect the acute tissue reaction to the faster degrading DAIII chitosan tubes, which argues against the use of those tubes for future trials.

Regarding the connective tissue surrounding the tube, no significant differences in thickness, area, numbers of multinucleated giant cells, and activated macrophages among the three DA groups were obvious. However, we detected a shift to a higher optical density of the unfolded connective tissue formed around DAIII chitosan tubes. Previously, it was reported that subcutaneously implanted chitosan scaffolds of different DAs induced different inflammatory responses which were more intense in the presence of materials with a DA of 15% as compared to materials with a DA of 4% [37]. In another study, chitosan membranes with different DAs were implanted under the calvarial periosteum and revealed as well different inflammation reactions [38]. Furthermore, chitosan sheets of different acetylation grades implanted into the spinal cord elicited different morphological reactions also in the nervous tissue [39]. In addition to different modes of fabrication of the chitosan devices, also the investigated implantation sites were different and could be the reason why in the present study varying reactions of the tube-surrounding connective tissue to the different DAs were minimized. Moreover, after 3 months only 1–2 remaining giant cells were found in the connective tissue preparations, which is the pattern of a reduced tissue response even seen at one year after the use of silicone tubes in nerve repair in humans, thus, the chitosan tubes can be judged as immunologically inert [5,40].

5. Conclusions

This comprehensive study provides a complex view on the suitability of fine-tuned chitosan tubes of different degree of acetylation to support peripheral nerve regeneration. With regard to the morphological and functional parameters of nerve regeneration, the chitosan tubes displayed a similar efficiency as the gold standard. However, differences were discovered regarding the immunological reaction, as well as other cellular processes, in the regenerative matrix and distal to the regenerated nerve and the chemical properties of tubes with the different DAs. While DAIII chitosan tubes (DA: ~20%) displayed a too fast degradation and induced degradation related tissue reactions, DAI tubes (DA: ~2%) induced an unintended sprouting effect in regenerating nerve fibres. Our findings point to DAII chitosan tubes (DA: ~5%) as the most supporting ones for peripheral nerve regeneration and as the first choice for ongoing applications in nerve reconstruction.

Acknowledgements

This work has received funding from the European Community's Seventh Framework Programme (FP7-HEALTH-2011) under grant agreement n° 278612 (BIOHYBRID).

We gratefully acknowledge the excellent technical assistance from the following people: members of the Institute of Neuroanatomy (Hannover Medical School): S. Fischer, N. Heidrich, K. Kuhlemann, J. Metzen and H. Streich; members of Università di Torino: S. Bompasso; and the guest researcher at Department of Clinical Sciences – Hand Surgery, Lund University, Dr A. Kodama from Hiroshima University, Hiroshima, Japan.

References

[1] Deumens R, Bozkurt A, Meek MF, Marcus MA, Joosten EA, Weis J, et al. Repairing injured peripheral nerves: bridging the gap. Prog Neurobiol 2010;92:245–76.
[2] Ray WZ, Mackinnon SE. Management of nerve gaps: autografts, allografts, nerve transfers, and end-to-side neurorrhaphy. Exp Neurol 2010;223:77–85.
[3] Battiston B, Raimondo S, Tos P, Gaidano V, Audisio C, Scevola A, et al. Chapter 11: tissue engineering of peripheral nerves. Int Rev Neurobiol 2009;87:227–49.
[4] Xu H, Yan Y, Li S. PDLLA/chondroitin sulfate/chitosan/NGF conduits for peripheral nerve regeneration. Biomaterials 2011;32:4506–16.
[5] Dahlin LB, Anagnostaki L, Lundborg G. Tissue response to silicone tubes used to repair human median and ulnar nerves. Scand J Plast Reconstr Surg Hand Surg 2001;35:29–34.
[6] Lundborg G, Rosen B, Dahlin L, Holmberg J, Rosen I. Tubular repair of the median or ulnar nerve in the human forearm: a 5-year follow-up. J Hand Surg Br 2004;29:100–7.
[7] Weber RA, Breidenbach WC, Brown RE, Jabaley ME, Mass DP. A randomized prospective study of polyglycolic acid conduits for digital nerve reconstruction in humans. Plast Reconstr Surg 2000;106:1036–45 discussion 46–8.
[8] Archibald SJ, Krarup C, Shefner J, Li ST, Madison RD. A collagen-based nerve guide conduit for peripheral nerve repair: an electrophysiological study of nerve regeneration in rodents and nonhuman primates. J Comp Neurol 1991;306:685–96.
[9] Archibald SJ, Shefner J, Krarup C, Madison RD. Monkey median nerve repaired by nerve graft or collagen nerve guide tube. J Neurosci 1995;15:4109–23.
[10] Bertleff MJ, Meek MF, Nicolai JP. A prospective clinical evaluation of biodegradable neurolac nerve guides for sensory nerve repair in the hand. J Hand Surg Am 2005;30:513–8.
[11] Hernandez-Cortes P, Garrido J, Camara M, Ravassa FO. Failed digital nerve reconstruction by foreign body reaction to Neurolac nerve conduit. Microsurgery 2010;30:414–6.
[12] Yuan Y, Zhang P, Yang Y, Wang X, Gu X. The interaction of Schwann cells with chitosan membranes and fibers in vitro. Biomaterials 2004;25:4273–8.
[13] Jiang X, Lim SH, Mao HQ, Chew SY. Current applications and future perspectives of artificial nerve conduits. Exp Neurol 2010;223:86–101.
[14] Dahlin LB, Lundborg G. Use of tubes in peripheral nerve repair. Neurosurg Clin N Am 2001;12:341–52.
[15] Freier T, Koh HS, Kazazian K, Shoichet MS. Controlling cell adhesion and degradation of chitosan films by N-acetylation. Biomaterials 2005;26:5872–8.
[16] Simoes MJ, Gartner A, Shirosaki Y, Gil da Costa RM, Cortez PP, Gartner F, et al. In vitro and in vivo chitosan membranes testing for peripheral nerve reconstruction. Acta Med Port 2011;24:43–52.
[17] Ao Q, Fung CK, Tsui AY, Cai S, Zuo HC, Chan YS, et al. The regeneration of transected sciatic nerves of adult rats using chitosan nerve conduits seeded with bone marrow stromal cell-derived Schwann cells. Biomaterials 2011;32:787–96.
[18] Freier T, Montenegro R, Shan Koh H, Shoichet MS. Chitin-based tubes for tissue engineering in the nervous system. Biomaterials 2005;26:4624–32.
[19] Hirai A, Odani H, Nakajima A. Determination of degree of deacetylation of chitosan by ^{1}H NMR spectroscopy. Polym Bull 1991;26:87–94.
[20] Salgado AJ, Coutinho OP, Reis RL. Novel starch-based scaffolds for bone tissue engineering: cytotoxicity, cell culture, and protein expression. Tissue Eng 2004;10:465–74.
[21] Salgado AJ, Gomes ME, Coutinho OP, Reis RL. Isolation and osteogenic differentiation of bone-marrow progenitor cells for application in tissue engineering. Methods Mol Biol 2004;238:123–30.

[22] Haastert-Talini K, Schmitte R, Korte N, Klode D, Ratzka A, Grothe C. Electrical stimulation accelerates axonal and functional peripheral nerve regeneration across long gaps. J Neurotrauma 2011;28:661–74.
[23] Cobianchi S, Casals-Diaz L, Jaramillo J, Navarro X. Differential effects of activity dependent treatments on axonal regeneration and neuropathic pain after peripheral nerve injury. Exp Neurol 2013;240:157–67.
[24] Rumpel R, Alam M, Klein A, Özer M, Wesemann M, Jin X, et al. Neuronal firing activity and gene expression changes in the subthalamic nucleus after transplantation of dopamine neurons in hemiparkinsonian rats. Neurobiol Dis 2013;59:230–43.
[25] Ratzka A, Kalve I, Ozer M, Nobre A, Wesemann M, Jungnickel J, et al. The co-layer method as an efficient way to genetically modify mesencephalic progenitor cells transplanted into 6-OHDA rat model of Parkinson's disease. Cell Transplant 2012;21:749–62.
[26] Saito H, Dahlin LB. Expression of ATF3 and axonal outgrowth are impaired after delayed nerve repair. BMC Neurosci 2008;9:88.
[27] Tsuda Y, Kanje M, Dahlin LB. Axonal outgrowth is associated with increased ERK 1/2 activation but decreased caspase 3 linked cell death in Schwann cells after immediate nerve repair in rats. BMC Neurosci 2011;12:12.
[28] Stenberg L, Kanje M, Dolezal K, Dahlin LB. Expression of activating transcription factor 3 (ATF 3) and caspase 3 in Schwann cells and axonal outgrowth after sciatic nerve repair in diabetic BB rats. Neurosci Lett 2012;515:34–8.
[29] Huelsenbeck SC, Rohrbeck A, Handreck A, Hellmich G, Kiaei E, Roettinger I, et al. C3 peptide promotes axonal regeneration and functional motor recovery after peripheral nerve injury. Neurotherapeutics 2012;9:185–98.
[30] Raimondo S, Fornaro M, Di Scipio F, Ronchi G, Giacobini-Robecchi MG, Geuna S. Chapter 5: methods and protocols in peripheral nerve regeneration experimental research: part II – morphological techniques. Int Rev Neurobiol 2009;87:81–103.
[31] Geuna S. Appreciating the difference between design-based and model-based sampling strategies in quantitative morphology of the nervous system. J Comp Neurol 2000;427:333–9.
[32] Yamaguchi I, Itoh S, Suzuki M, Osaka A, Tanaka J. The chitosan prepared from crab tendons: II. The chitosan/apatite composites and their application to nerve regeneration. Biomaterials 2003;24:3285–92.
[33] Costa-Pinto AR, Salgado AJ, Correlo VM, Sol P, Bhattacharya M, Charbord P, et al. Adhesion, proliferation, and osteogenic differentiation of a mouse mesenchymal stem cell line (BMC9) seeded on novel melt-based chitosan/polyester 3D porous scaffolds. Tissue Eng Part A 2008;14:1049–57.
[34] Zhao Q, Lundborg G, Danielsen N, Bjursten LM, Dahlin LB. Nerve regeneration in a 'pseudo-nerve' graft created in a silicone tube. Brain Res 1997;769:125–34.
[35] Schmidt CE, Leach JB. Neural tissue engineering: strategies for repair and regeneration. Annu Rev Biomed Eng 2003;5:293–347.
[36] Streppel M, Azzolin N, Dohm S, Guntinas-Lichius O, Haas C, Grothe C, et al. Focal application of neutralizing antibodies to soluble neurotrophic factors reduces collateral axonal branching after peripheral nerve lesion. Eur J Neurosci 2002;15:1327–42.
[37] Barbosa JN, Amaral IF, Aguas AP, Barbosa MA. Evaluation of the effect of the degree of acetylation on the inflammatory response to 3D porous chitosan scaffolds. J Biomed Mater Res A 2010;93:20–8.
[38] Hidaka Y, Ito M, Mori K, Yagasaki H, Kafrawy AH. Histopathological and immunohistochemical studies of membranes of deacetylated chitin derivatives implanted over rat calvaria. J Biomed Mater Res 1999;46:418–23.
[39] Yussof SJM, Halim AS, Saad AZM, Jaafar H. Evaluation of the biocompatibility of a bilayer chitosan skin regenerating template, human skin allograft, and integra implants in rats. ISRN Mater Sci 2011;2011:7.
[40] Brodbeck WG, Anderson JM. Giant cell formation and function. Curr Opin Hematol 2009;16:53–7.